

TUTORIAL REVIEW

View Article Online



Cite this: Chem. Soc. Rev., 2021, **50**, 10743

From bulk to interface: electrochemical phenomena and mechanism studies in batteries via electrochemical quartz crystal microbalance

Yuchen Ji,†a Zu-Wei Yin, p†*a Zhenzhen Yang, Ya-Ping Deng, pc Haibiao Chen, d Cong Lin, Luyi Yang, Lai Yang, Mingjian Zhang, Qiangfeng Xiao, Jun-Tao Li, Chongwei Chen, Chen,

Understanding the bulk and interfacial behaviors during the operation of batteries (e.g., Li-ion, Na-ion, Li-O₂ batteries, etc.) is of great significance for the continuing improvement of the performance. Electrochemical quartz crystal microbalance (EQCM) is a powerful tool to this end, as it enables in situ investigation into various phenomena, including ion insertion/deinsertion within electrodes, solid nucleation from the electrolyte, interphasial formation/evolution and solid-liquid coordination. As such, EQCM analysis helps to decipher the underlying mechanisms both in the bulk and at the interface. This tutorial review will present the recent progress in mechanistic studies of batteries achieved by the EQCM technology. The fundamentals and unique capability of EQCM are first discussed and compared with other techniques, and then the combination of EQCM with other in situ techniques is also covered. In addition, the recent studies utilizing EQCM technologies in revealing phenomena and mechanisms of various batteries are reviewed. Perspectives regarding the future application of EQCM in battery studies are given at the end.

Received 2nd July 2021

DOI: 10.1039/d1cs00629k

rsc.li/chem-soc-rev

Key learning points

- (1) Fundamentals of the EQCM technique, such as theory and operational principles (gravimetry and beyond), historical overview, widespread applications in
- (2) Unique advantages of EQCM in battery studies and typical combinations with other in situ techniques.
- (3) The utilization of EOCM in recent studies on bulk phenomena and interfacial mechanisms of batteries.
- (4) Perspectives regarding the application of EQCM for future battery studies.
- (5) Potential applications of EQCM for the chemistry field involving (de)adsorption, corrosion/dissolution, nucleation, (de)insertion, (de)alloying, solid-liquid coordination, etc.

^a School of Advanced Materials, Peking University, Shenzhen Graduate School, Shenzhen 518055, China. E-mail: yinzuwei@pku.edu.cn, panfeng@pkusz.edu.cn

 f State Key Lab of Physical Chemistry of Solid Surface, College of Chemistry and Chemical Engineering, Xiamen University, Xiamen 361005, China

1. Introduction

Rechargeable batteries (e.g., lithium/sodium/magnesium ion batteries, lithium-sulfur batteries, Li-O2 batteries, etc.) have become the foremost means for the storage of electric power. Rechargeable batteries are widely used as power sources in portable electronics (e.g., laptop computers, cell phones, smart wearables, etc.), electric vehicles, and grid power storage.¹ Energy density, power density, charge-discharge rate, cost, cycle life, safety, and environmental impact are some parameters that need to be considered in the selection of battery technology for specific applications. For instance, although energy density is one of the most critical aspects for portable electronics, safety, cost, and cycling stability are equally important for electric vehicles. The cost, cycle life, and safety become

^b Chemical Sciences and Engineering Division, Argonne National Laboratory, 9700 S Cass Ave, Lemont, IL, 60439, USA

^c Department of Chemical Engineering, Waterloo Institute for Nanotechnology, Waterloo Institute for Sustainable Energy, University of Waterloo, Waterloo, Ontario N2L 3G1, Canada

^d Institute of Marine Biomedicine, Shenzhen Polytechnic, Shenzhen 518055, China

^e School of Automotive Studies & Clean Energy Automotive Engineering Center, Tongji University (Jiading Campus), 4800 Cao'an Road, Shanghai 201804, China

[†] Y. Ji and Z.-W. Yin contributed equally to this work.

Tutorial Review Chem Soc Rev

more important than energy density for grid-energy storage. The capability of being charged and discharged quickly is desirable for most applications. All these performance parameters are largely determined by the components in the battery, including the electrodes (cathode and anode), electrolyte, interface, binder, current collectors, and separator.

To pursue high-performance batteries, great efforts have been made to select and match the right components, to develop new materials, and to improve the fabrication engineering.1 However, the electrochemical processes occurring during charging-discharging of a battery are complicated and involved phenomena in the bulk phases of the electrodes, electrolyte and at the interface between the electrodes and the electrolyte. The mechanisms governing these phenomena need to be elucidated in depth to effectively enhance the performance. Essential phenomena dictating the performance of a battery include: ion (de)insertion in the electrodes, nucleation of solids derived from the electrolyte, formation/evolution of



Yuchen Ji

Yuchen Ji is currently a PhD candidate at Peking University, Shenzhen Graduate School under the supervision of Prof. Feng Pan. Не received his bachelor's degree from Beijing University of Technology in 2019. His research focuses on the in situ advanced characterization of the electrolyte and interface evolution in lithium batteries, including in situ AFM, EQCM, etc.

the electrode/electrolyte interphase and solid-liquid coordination. A better knowledge on one or more of these specific phenomena is of great significance to guide the selection of battery components and the improvement of battery production engineering.

In recent years, advanced characterization techniques have greatly facilitated the studies of electrochemical phenomena and mechanisms in batteries.^{2,3} With the development of various techniques (i.e. transmission electron microscope (TEM), atomic force microscope (AFM), X-ray absorption spectroscopy (XAS), etc.), the structure, morphology and chemical composition can be well investigated statically or dynamically. Among all the emerging technquies, electrochemical quartz crystal microbalance (EQCM) is a relatively cheap and non-destructive characterization method, and it can provide in situ information on the mass change and reflect the evolution of the structure both in the bulk and at the surface of battery electrodes. 4,5 In addition, the preparation of specimens for EQCM is quite simple, and the specimen can largely simulate the behavior of a real electrode. Thus, EQCM is a powerful tool to study the electrochemical phenomena and mechanisms in batteries.

In this review, we first go over the current status of common characterization techniques and the basics of EQCM, including the unique capability, background (e.g., the theory and principles of operation, historical overview, etc.), benefits to battery studies, and combinations with other in situ techniques (e.g., X-ray diffraction (XRD), AFM, differential electrochemical mass spectrometry (DEMS), etc.). In addition, the recent works on applying EQCM (gravimetric and beyond) for the study of phenomena in the bulks of the electrodes and electrolyte and the interfacial reaction mechanisms are further reviewed. As illustrated in Fig. 1, specifically, the bulk phenomena include



Zu-Wei Yin

Dr Zu-Wei Yin received his PhD degree from the College of Energy at Xiamen University in 2019 under the supervision of Prof. Shi-Gang Sun. He was a joint PhDstudent at Lawrence Berkeley National Lab (U.S.) between 2016 and 2019 under the supervision of Prof. Haimei Zheng. Dr Yin is currently a Postdoc Schoolat theAdvanced Materials, Peking University Shenzhen Graduate School. His research interests

mainly focus on the electrochemical reaction mechanisms in batteries, catalysis and advanced characterization techniques, such as EQCM, TEM, XAS, etc.



Feng Pan

Prof. Feng Pan, Chair-Professor, VP Peking University Shenzhen Graduate School, Founding Dean of School of Advanced Materials, Director of National Center of Electric Vehicle Power Materials for **Battery** and International Research, received BSdegree from Dept. Chemistry, Peking University in 1985 and PhD from Dept. of P&A Chemistry, University of Strathclyde, U.K. with "Patrick D. Ritchie Prize" for the best

PhD in 1994. Prof. Pan has been engaged in fundamental research of structure chemistry, exploring "Material Gene" for Liion batteries and developing novel energy conversion-storage materials & devices. He also received the 2018 ECS Battery Technology Award (US), and 2021 Electrochemistry Contribution Award.

Chem Soc Rev **Tutorial Review**

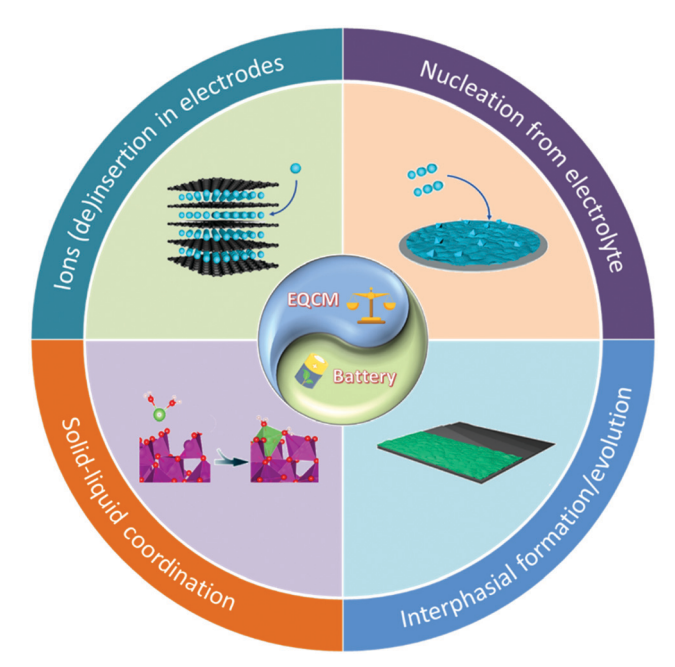


Fig. 1 Schematic illustration of application areas of the EQCM in battery research

ion (de)insertion behavior in the electrodes (e.g., charge storage mechanism, electrode structural evolutions, and electrochemical ion-exchange synthesis, etc.) and nucleation derived from the electrolyte (e.g., ion electro-deposition on alkali metal anodes, nucleation on metal-O₂ battery cathodes, etc.). The interfacial reactions include the formation/evolution of the solid electrolyte interphase (SEI) (e.g., on inert electrodes and active batteries electrodes), and solid-liquid coordination. Finally, we give our perspectives on future research and development for utilizing EQCM for battery studies.

2. The current status of characterization techniques

The electrochemical phenomena and mechanisms in batteries, including those in the bulk and at the interface, have been widely investigated by various characterization techniques. However, there are some limitations with these commonly applied characterization tools.

For the study of ion (de)insertion behavior in the electrodes, nuclear magnetic resonance (NMR) and electrochemical protocols such as the galvanostatic intermittent titration technique (GITT) and potentiostatic intermittent titration technique (PITT) are employed to measure the diffusion rates of metal ions (Li⁺, Na⁺, Mg²⁺, etc.). Scanning tunnel microscopy (STM) and AFM have been adopted to visualize the static and dynamic surface morphology at the nano/atomic level. Several other characterization methods have been applied to reveal the changes in the properties of the electrode before and after the insertion/extraction process. For example, TEM and scanning electron microscopy (SEM) can reveal the change in the morphology, and XRD as well as neutron diffraction (ND) can analyze the structural evolution in the bulk. 2,3 Nevertheless, the diffusion rates of metal ions during charge-discharge are difficult to obtain in real time by NMR, GITT, or PITT. STM and AFM can only gain information from the surface, and the samples for observation need to be prepared to expose a smooth and flat surface, which are quite different from the electrode in actual batteries. Most of the TEM, SEM, XRD, and ND techniques lack the capability of characterization in real time when the ions insert/extract during the charge-discharge process. Some techniques can be modified for in situ analysis, such as in situ AFM, in situ TEM, etc., but the sample preparation standards and measuring conditions are quite strict, making the characterization operations complicated.

To study the nucleation of solids from the electrolyte, which mainly involves the electrodeposition on the alkaline metal anodes and the formation/evolution of lithium oxide in Li-O2 batteries, there are very limited reports on in situ characterization methods (e.g., XRD and TEM).^{2,3} Due to the sensitivity of the alkali metals (e.g. Li, Na, etc.) and the intermediates in Li-O₂ batteries upon incident radiations (e.g., electrons, X-ray, etc.), it is difficult to observe their nucleation processes using characterization tools like TEM, XAS, XRD, electron energy loss spectroscopy (EELS), etc. The current results obtained by ex situ and in situ measurements on the nucleation process may not be accurate.

For the formation/evolution of electrode/electrolyte interphase, many analytical tools have been applied to determine the chemical composition and the formation mechanism.³ These tools include, X-ray-based (X-ray photoelectron spectroscopy (XPS), XAS, X-ray scattering and image, etc.), electronbased (SEM, TEM, EELS, etc.), scanning probe-based (AFM, STM, etc.), and vibrational analytical (Fourier transform infrared spectroscopy (FTIR), Raman, etc.) techniques. However, incident X-rays and electrons can induce changes in the interfacial films. Only the average surface information can be obtained when X-ray-based, electron-based, and vibrational analytical tools are adopted. The limitation of scanning probe-based techniques is that they can only produce reasonable results by scanning ideally flat electrodes, which are distinctly different from practical electrodes.

For solid-liquid coordination, only very few methods, such as surface enhanced Raman spectroscopy (SERS) and FTIR, were successfully applied to detect the interfacial structure.³ Performing in situ measurements at the interface is in demand, but it is also difficult due to the complicated environment in batteries, especially during the operational processes.

Fundamentals of the EQCM technique

3.1 Theory and operational principle EQCM

EQCM can provide electrochemical and gravimetric information in real time by combining traditional quartz crystal microbalance (QCM) with electrochemical technologies in a solid/ Tutorial Review Chem Soc Rev

liquid system.⁶ QCM is an ultra-sensitive weight detector with sensitivity at the level of nano-grams and it operates based on the inverse piezoelectric effect of a quartz crystal and the change of the resonant frequency due to the change in the mass of the specimen.

As depicted in Fig. 2, there are three core components in a typical EQCM setup: a quartz crystal chip, an oscillator and an electrochemical workstation (potentiostat). The quartz crystal chip is used as the sensor and the working electrode of the system, and it oscillates at the resonant frequency during the measurements. The quartz crystal chip usually comprises a thin AT-cut quartz crystal sheet and a metal (Au, Pt, Cu, etc.) layer sprayed on both sides of the quartz sheet serving as the electrode. Among various types of sprayed metals, gold (Au) has become the optimal option for many applications, due to its easy microscale formation using common semiconductor processing techniques. For battery studies, an electrode material can be coated on the Au layer. The resonance frequency of the electrode changes with the change in the mass of the electrode due to the occurrence of an electrochemical process. The oscillator records the change of the frequency and the impedance of the quartz crystal. An electrochemical workstation is used for conducting electrochemical tests, such as cyclic voltammetry (CV) and galvanostatic charge-discharge.

Fig. 3 displays a brief history of the development of the EQCM technique. The design of EQCM originated from the inverse piezoelectric effect discovered by the Currie brothers in 1880:⁶ when the quartz crystal is placed in an alternating electric field with a frequency similar to the natural frequency of the quartz crystal, a resonant stationary wave will be generated inside the quartz crystal. In general, AT-cut quartz crystals operating in the thickness-shear mode are used in EQCM, and the condition for maintaining an internal stationary wave is as follows:⁶

$$f_0 = V_{\rm tr}/2t_{\rm q} = (\mu_{\rm q}/\rho_{\rm q})^{1/2}/2t_{\rm q}$$
 (1)

wherein, f_0 is the fundamental frequency of the quartz crystal, $V_{\rm tr} = (\mu_{\rm q}/\rho_{\rm q})^{1/2}$ is the propagation speed of the sound wave in

the quartz crystal, $\mu_{\rm q}$ and $\rho_{\rm q}$ are the modulus and density of the quartz crystal, respectively, and $t_{\rm q}$ is the thickness of the quartz crystal.

If a uniform layer of a heterogeneous material is rigidly attached to the surface of the quartz crystal, the stationary wave will pass through the interface between the two materials and propagate in the outer adherent layer. Assuming that the external adherent layer has the same shear modulus and density as the quartz crystal, the change in the frequency Δf caused by the presence of the adherent layer (thickness D_t) follows the equation as below:

$$\Delta f/f_0 = -D_t/t_q = -2f_0D_t/V_{tr}$$
 (2)

Thus the Sauerbrey equation can be obtained from eqn (1) and (2):

$$\Delta f = -\left[2f_0/A(\mu_{\rm q}/\rho_{\rm q})^{1/2}\right] \cdot \Delta m = -C_{\rm f} \cdot \Delta m \tag{3}$$

where A is the piezoelectrically active area, Δm is the mass change per unit area, and $C_{\rm f} = 2f_0/A(\mu_{\rm q}/\rho_{\rm q})^{1/2}$ is called the mass sensitivity of QCM. This equation is the basic principle of QCM in a gas atmosphere and it was derived by Sauerbrey in 1959.⁷ The Sauerbrey equation works nicely when $\Delta f/f_0 < 2\%$.

In electrochemical systems, the mass change is often caused by redox reactions, so researchers are concerned about the relationship between the electrochemical parameters and the frequency change measured by QCM. Thus another parameter commonly used in the EQCM test can be obtained: MPE (mass accumulated per mole of electron transferred), which is calculated according to the Faraday's law.⁶

$$MPE = nF \cdot \Delta m/Q \tag{4}$$

Combining eqn (3) and (4), the following formula can be obtained:

$$MPE = -nC_f F \cdot \Delta f/Q \tag{5}$$

where Q presents the charge through the electrode, n is the valence state of reaction ions, and F is the Faraday constant (96 485 C mol⁻¹). A typical CV curve and the corresponding

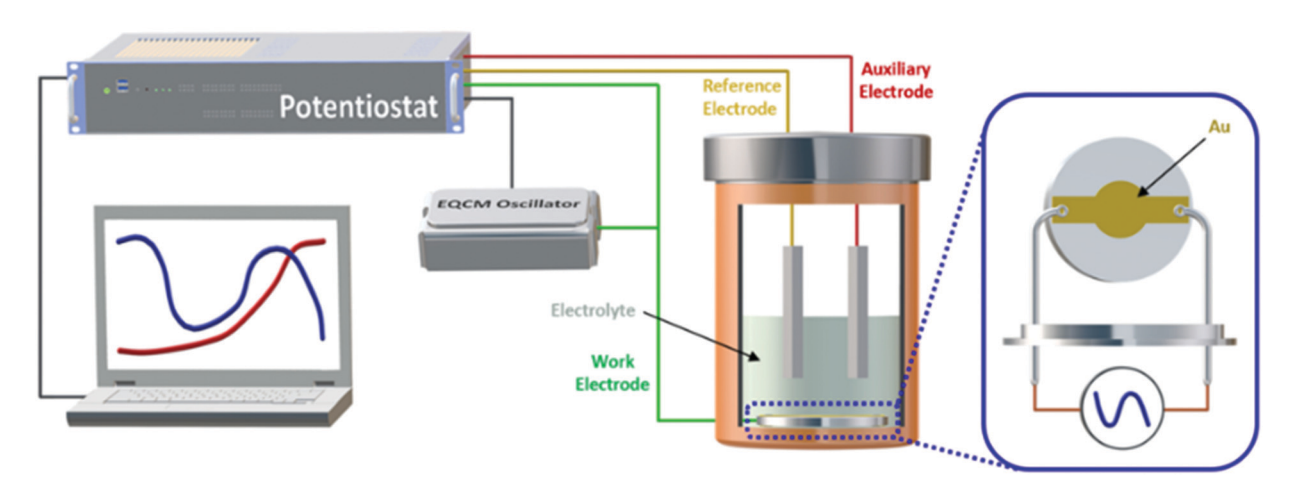


Fig. 2 Scheme of a typical EQCM experimental setup for studying rechargeable batteries.

Key study objects EQCM technique development

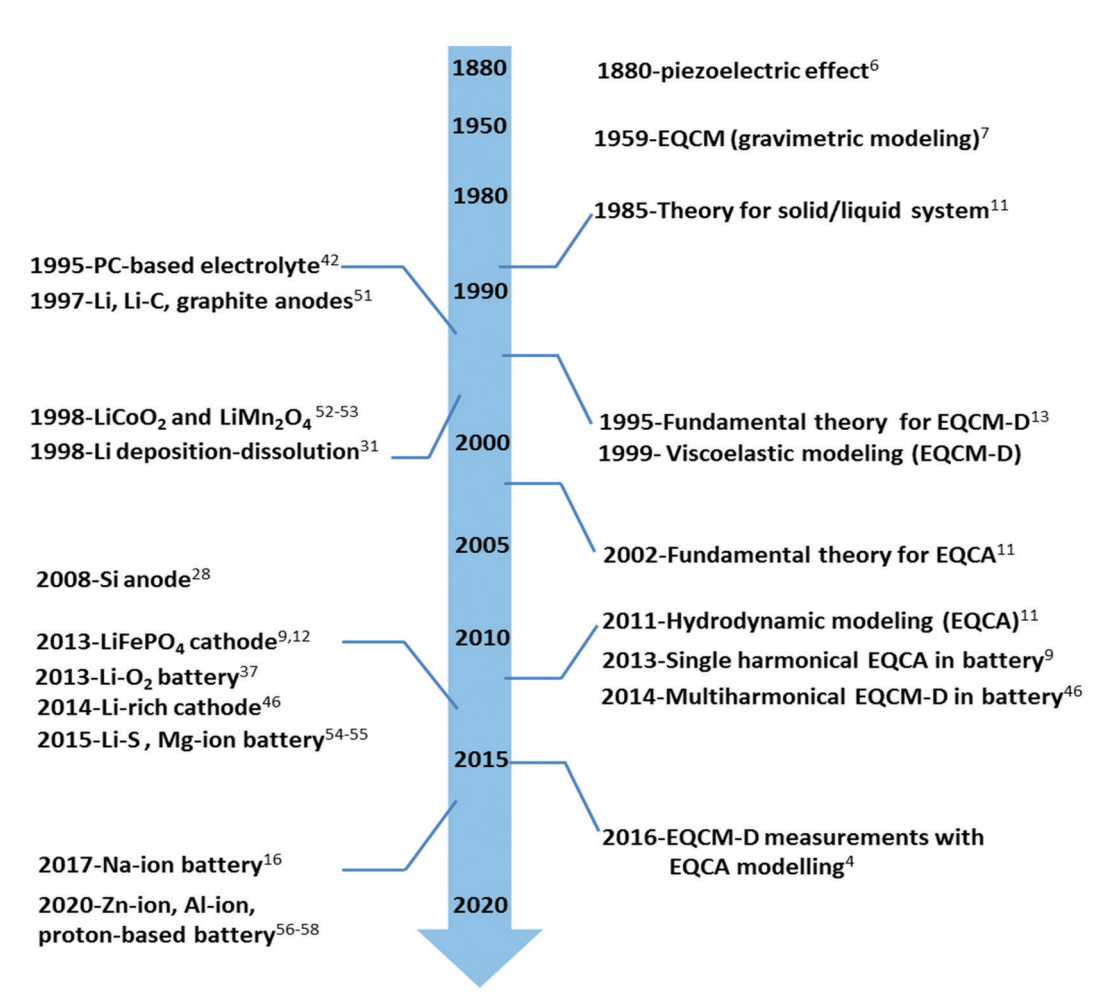


Fig. 3 Scheme showing a historical overview of EQCM technique development. 4,6,7,9,11-13,16,28,31,37,42,46,51-58

mass change of a graphite electrode during EQCM measurement are shown in Fig. 4a.5 The black line is the negative scan of the CV curve during discharge of graphite, and the blue line is the corresponding mass change calculated from the frequency change of the electrode. The current peak in the region VI (black line) indicates that the lithiation of graphite, and an obvious corresponding mass increase can be observed (blue line). And a typical mass-charge curve showing the calculation of the MPE value is displayed in Fig. 4b.8

EQCM techniques beyond gravimetry

The Sauerbrev equation has the limitation that it is only appropriate for rigid films, and the effect of a liquid medium has not been considered. For more complicated viscoelastic solid/liquid systems, there is a need of developing new models. In 1985, Kanazawa et al. theoretically analyzed the frequency shift induced by the change in the density (ρ_L) and viscosity (η_L) of the liquid in contact with the quartz crystal electrode. 11 Such a liquid-induced factor cannot be ignored in many solid/liquid systems. The obtained equation is as follows:

$$\Delta f_{\rm L} = f_0^{3/2} [\eta_{\rm L} \rho_{\rm L} / (\pi \mu_{\rm q} \rho_{\rm q})]^{1/2}$$
 (6)

where, $\Delta f_{\rm L}$ is the frequency shift caused by the liquid, while $\eta_{\rm L}$ and $\rho_{\rm L}$ are the viscosity and density of the adhering liquid on the quartz crystal surface, respectively. When considering the liquid-induced factor, the measured frequency change Δf is the sum of the frequency variation associated with the loss or gain of the mass $(\Delta f_{\rm m})$ and the change in $\Delta \eta_{\rm L} \rho_{\rm L}$ of the liquid $(\Delta f_{\rm L})$ during the electrochemical process:

$$\Delta f = \Delta f_{\rm m} + \Delta f_{\rm L} \tag{7}$$

 $\Delta(\eta_{\rm L}\rho_{\rm L})$ can be estimated from the change in the impedance of the quartz crystal (ΔR) , ¹¹

$$\Delta R = [2\pi f_0 \Delta (\eta_{\rm L} \rho_{\rm L})]^{1/2} A/k^2 = -[\pi (2\mu_{\rm q} \rho_{\rm q})^{1/2} A/(k^2 f_0)] \Delta f_{\rm L}$$
 (8)

where k is the electromechanical factor. From eqn (8), it can be seen that $\Delta f_{\rm L}$ has a negative linear correlation with ΔR . That is, an increase of ΔR means a decrease of $\Delta f_{\rm L}$.

To quantitatively analyze a viscoelastic solid/liquid system, energy dissipation (D) was introduced into the model and Tutorial Review Chem Soc Rev

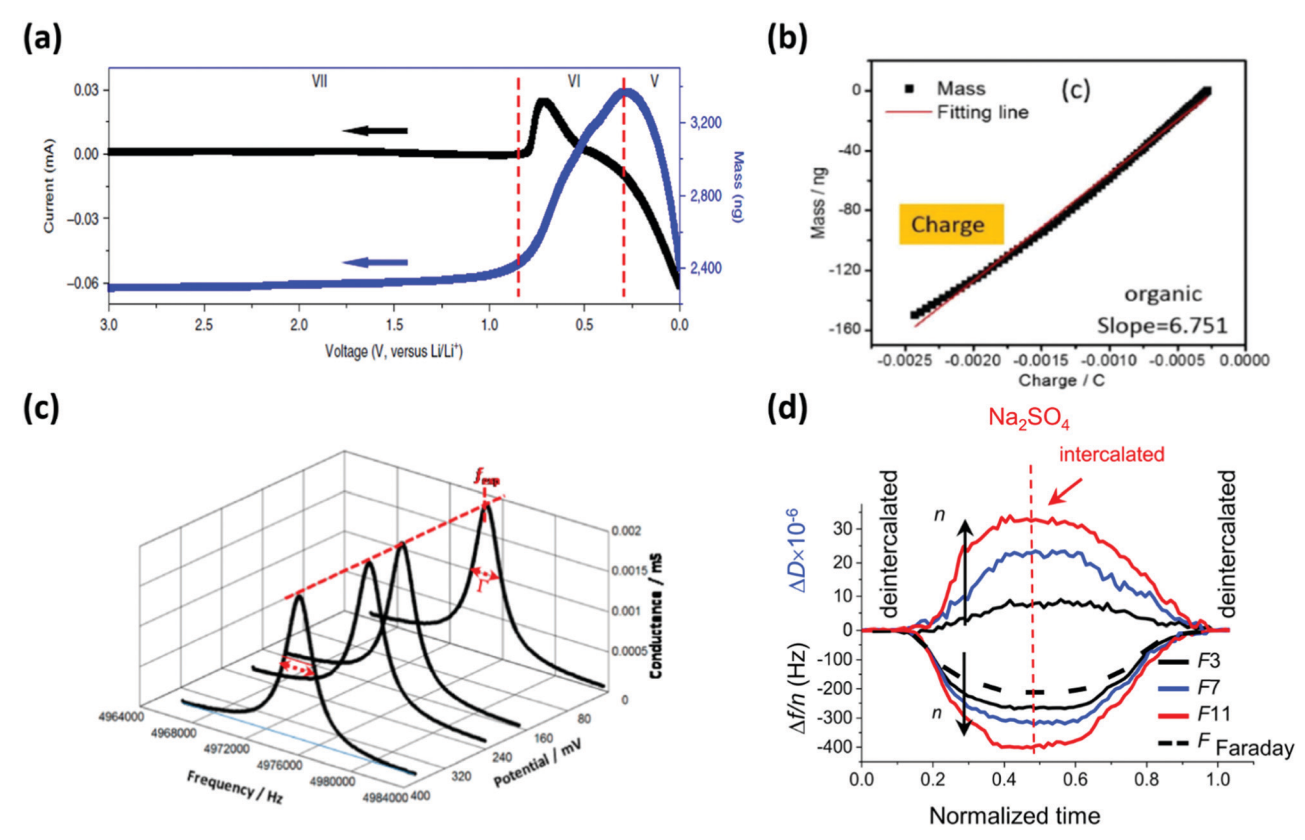


Fig. 4 Typical EQCM measurement data. (a) CV curve and corresponding mass change, Reproduced from ref. 5 with permission from Springer Nature, Copyright 2018. (b) Mass—charge curve showing the calculation of MPE value. Reproduced from ref. 8 with permission from Elsevier, Copyright 2017. (c) Resonance peaks measured at different potentials by EQCA. Reproduced from ref. 9 with permission from American Chemical Society, Copyright 2013. (d) Time-dependent changes in $\Delta f/n$ and ΔD for the different overtone orders during a complete cycle measured *via* EQCM-D. Reproduced from ref. 10 with permission from Elsevier, Copyright 2018.

measured experimentally. There are two popular approaches to find the information about the change in energy dissipation (D) due to the adsorption of a viscoelastic film. One is impedance analysis by measuring the width of the resonance peak while damping the crystal (Fig. 4c), and this method was proposed in 2002 and initially called quartz crystal admittance (QCA). For batteries, this method provides a direct assessment of the potential-driven frequency shifts ($\Delta f_{\rm exp}$) and changes in the resonance peak width ($\Delta \Gamma$ or ΔW) during charge–discharge.

 $\Delta f_{\rm exp}$ and $\Delta \Gamma$ (ΔW) could further be used to make $\Delta f_{\rm exp} - \delta$ and $\Delta W - \delta$ curves, in which δ is the penetration depth of the shear wave emitted by oscillating quartz crystals towards the surrounding viscous liquid, as follows:^{4,11}

$$\delta_n = \left[\eta_{\rm L} / \pi n \rho_{\rm L} f_0 \right]^{1/2} \tag{9}$$

where, δ_n is the penetration depth at an overtone of n. For an ideally flat electrode, Δf and ΔW has a linear relationship with δ_n :¹¹

$$(\Delta f/n)/(n\rho_{\rm L}f_0^2) = -\delta_n/(\mu_{\rm q}\rho_{\rm q})^{1/2}$$
 (10)

$$(\Delta W/n)/(2n\rho_{\rm L}f_0^2) = \delta_n/(\mu_{\rm G}\rho_{\rm G})^{1/2}$$
 (11)

But for electrodes with a rough surface or porous structure, the $\Delta f_{\rm exp} - \delta$ and $\Delta W - \delta$ curves will deviate from a linear

relationship. The analyses of such curves can be used to determine the structure (*i.e.* morphology, roughness, *etc.*) of electrodes. Levi and co-workers firstly proposed the single-harmonic (n = 1) hydrodynamic model of EQCM for batteries, integrating carbon particles and PVDF binder in the model composite electrode.¹¹ Then they employed the hydrodynamic model to track the ion insertion into LiFePO₄ in aqueous solutions,⁹ and the intercalation-induced phase transitions of the LiFePO₄ electrode.¹² In their reports, they termed this technique electrochemical quartz crystal admittance (EQCA).

The other approach is to monitor the decay in the oscillation of the crystal after a rapid pulse of excitation close to the resonant frequency. The principle for this approach is to switch on and off the driving alternating current (AC) voltage periodically to measure the energy loss of the quartz into the surrounding environment. The dissipation factor (*D*) is calculated according to the following equation derived by Rodahl *et al.* in 1995^{11,13}

$$D = E_{\text{dissipated}} / 2\pi E_{\text{stored}} = 1 / f \pi \tau$$
 (12)

where $E_{\rm stored}$ is the initial energy of the sensor and $E_{\rm dissipated}$ is the energy lost during a single oscillation after removing the driving voltage. The amplitude decays with time depending on the properties of the oscillator and the contacting medium at

Chem Soc Rev **Tutorial Review**

the surface. Such a viscoelastic modelling can be used to analyze the mechanical changes of the electrodes.

Generally speaking, a high *D* is obtained when the chip loses its energy quickly, implying that the adsorbate on the sensor surface is viscous (soft) and thick. Conversely, a low D suggests that the adsorbed species on the surface is rigid and compact. Furthermore, it is possible by EQCM with a dissipation (EQCM-D) approach to probe f and D values at multiple harmonics of a resonant frequency (e.g., n = 3, 5, 7... for 5 MHz) on the millisecond time scale. Combining data obtained from f and D measurements at different overtones (n) along with an appropriate model can provide information about the changes in not only the mass but also the viscoelastic characteristics of the adherent surface film, both quantitatively and qualitatively (Fig. 4d). A company, Qsense, commercialized this technique in 1999. Since then, many studies regarding the mass, thickness, shear viscosity and storage modulus at the solid-liquid interface in biochemical and electrochemical systems have been reported. Levi and co-workers furtherly introduced a new comprehensive methodology based on multiharmonic EQCM-D measurements, followed by hydrodynamic EQCA modelling.⁴ The following equation was derived from the model:

$$\Delta D = (\Delta W/n)/(\Delta f/n) \tag{13}$$

The novel EQCM-D technique can obtain three vital parameters (Fig. 4d): $\Delta f/n$ (frequency on multiple harmonics), $\Delta W/n$ (resonance width on multiple harmonics), and δ_n (penetration depth). Levi and co-workers validated the new EQCM-D technique with hydrodynamic probes in two cases: the first is an ideally flat Au-covered quartz crystal immersed in water and water-glycerol mixtures; the second is an artificially roughened surface composed of lithographically fabricated polymeric photoresist hemi-spheres in contact with water. Then they applied this model to study many battery phenomena. 4,9,12,14

3.3 Widespread applications of EQCM in the chemistry field

Based on the working principle, EQCM is wildely applied in different fields of chemistry related to the electrochemical reactions and electrode variations, such as electrocatalysis, (photo)electrocatalysis, supercapacitors, batteries, corrosion electrochemistry, electrodeposition, bioelectrochemistry, etc. 6,15 These branch fields involve complicated bulk and/or interfacical reactions driven by electrochemistry, which inevitably lead to a subtle change in mass. Thus, EQCM is an appropriate characterization tool to in situ reveal the evolution mechanism during the whole working process. For instance, EQCM can accurately detect the adsorption and desorption behaviors during an electrocatalytic process or charging/discharging of a supercapacitior. Moreover, electrodeposition and electrochemical corrosion can be quantitatively studied via EQCM, as the mass change generated by the ion deposition and stripping at the solid-liquid interface can be accurately recorded.

However, among the whole electrochemistry field, batteries seem to be the most complicated systems, because the different behaviors during the charging-discharging processes are not only involved in the bulk processes (ion insertion and deinsertion in electrodes, nucleation, etc.), but also related to the interfacial reaction and reconstruction (interphasial evolution, solid-liquid coordination, etc.). The intricate reactions bring big challenges to the tranditional characterization methods to study the energy storage mechanism of different batteries. Nevertheless, electrode mass change, an important physical quantity delivering very useful information, is often ignored. Different electrochemical behaviors cause different reaction products causing corresponding mass variations. EQCM can in situ detect these specific mass changes to study the reaction mechanisms if it is employed properly under particular conditions. Reviewing and summarizing the applications of EQCM studies on battery phonemena is of great significance to both battery and EQCM development, i.e. searching for novel methods to explore battery mechanisms from bulk to surface at different scales and novel application fields of the EQCM method, etc.

4. Applications of EQCM in battery studies

4.1 Benefits of using EQCM to study batteries

As shown in the left side of Fig. 3, EQCM was first applied for battery studies in 1995. It has been used to study different electrolytes, cathodes, anodes, and novel battery types (e.g., Li-S, Na-ion, Mg-ion, Li-O2, etc.). EQCM facilitates the battery studies in the following aspects.

For the ion (de)insertion behavior, EQCM can in situ detect changes in mass and charge induced by ion transport, providing opportunities to clarify the controversial reaction mechanisms during ion insertion/extraction. For example, EQCM studies have been applied to explain the details about the anion redox mechanism of battery cathodes at high voltages (>4.4 V vs. Li/Li⁺), co-insertion behavior of solvent molecules with metal ions (e.g., the potential/electrolyte effect, solvation number, etc.), and intermediate states during alloying/ de-alloying of the anode materials. The charge storage mechanism of emerging novel electrode materials and electrochemical synthesis involving ion-exchange can also be investigated by EQCM. In addition, the advanced EQCM-D can provide information in situ on the change in the structure of the battery materials, such as phase transformation, surface morphology evolution (e.g., roughness), volume changes (i.e., strain), etc. 11

For studying the nucleation of solids from the electrolyte, the non-damaging EQCM was mainly used to investigate the formation of the intermediate species during the electro-deposition of alkali-metals and the reactions at the cathode of Li-O₂ batteries. EQCM provides accurate measurements on the potential, MPE value and mass change with different electrolytes. In addition, the data can also be used to accurately determine the chemical compositions of the intermediate species when combined with other in/ex situ structural and compositional characterization methods (e.g., XRD, XPS, EDS, etc.).

Tutorial Review Chem Soc Rev

Table 1 Typical combinations of EQCM with other in situ techniques for battery studies

No.	Combined techniques	Study objects	Specific research points	Ref.
1	In situ AFM	LiMn ₂ O ₄	Intercalation-induced volume change of crystalline material	
2	In situ XRD, EC-STM	Graphite	Intercalation of solvated Na-ions	Seidl et al. 16
3	<i>In situ</i> Raman	Li–O ₂ battery	Effect of water and HF on discharge products	Tomita et al. ¹⁷
4	In situ AFM	Na-O ₂ battery	Shuttling effect of redox mediator on discharge products	Pan <i>et al.</i> ²⁰
5	In situ FTIR, AFM, EIS	Alkyl carbonates/Li salt electrolytes	SEI on noble-metal electrodes	Aurbach <i>et al.</i> ¹⁸
6	In situ AFM and DEMS	Graphite	SEI formation/evolution mechanism	Pan <i>et al.</i> ⁵
7	In situ EIS	Li-rich cathode	Li ₂ MnO ₃ activation and CEI evolution	Yin et al. 19

For the interphasial formation/evolution, EQCM can measure in situ mass change, as well as the electrochemical and structural properties of the interfacial films. The advantages of being non-damaging, sensitive to both bulk and surface change, and capable of simulating real-life electrodes make EQCM a unique tool. Moreover, for multi-layer interphasial formation/evolution processes, EQCM can provide accurate potentials at the beginning and end of the growth for different layers.

For the solid-liquid coordination, EQCM is a facile method to provide the mass, charge, and MPE information during the interfacial reconstruction. Practical battery samples can be used, and the preparation and operation of electrochemical tests can also be achieved easily.

4.2 Combination of EQCM with other in situ techniques

Although EQCM exhibits irreplaceable advantages and can provide unique information for battery studies, it is limited to measurement of the structure, morphology and physicochemical changes. Thus, the combination of EQCM with other in situ techniques (e.g., XRD, STM, SEM, AFM, MS, FTIR, Raman, EIS, etc.) can take advantage of different techniques and provide comprehensive insights into the charge-discharge mechanism of batteries. For example, a combination of EQCM and in situ XRD can investigate the ion insertion/extraction mechanism, especially for co-intercalation with solvents;¹⁶ combination of EQCM with in situ Raman is an effective method for studying the electrode-electrolyte interactions, including the electrolyte decomposition product and the reactions on the oxygen cathode of Li-O2 batteries; 17 EQCM and simultaneous electrochemical impedance spectroscopy (EIS), AFM, STM, FTIR, XPS, etc. are useful for interfacial observations. 5,18,19 Table 1 summarizes the typical battery studies in open literature reports combining EQCM and other in situ techniques.

5. Bulk phenomena studies

Ion (de)insertion in electrodes

5.1.1 Charge storage mechanism. The basic working principle of rechargeable batteries is the reversible insertion/extraction of inorganic ions (i.e. Li⁺, Na⁺, PF₆⁻, etc.) in/out of the electrode material, which is often referred to as "rocking-chair" behavior. To improve the performance of Li-ion batteries, it is desirable to store more Li⁺ in the cathode and anode materials and ensure the stability of Li⁺ extraction/insertion processes

simultaneously. However, innovations in these electrode materials are hindered due to the difficulty in revealing the ion storage mechanism. This is because the ion insertion/extraction processes of the electrode involve concurrent ionic and electronic transport through the electrodes, within the electrolyte, and at their interfaces. EQCM is an in situ characterization technique to detect the mass change of the electrode per mole of electrons transferred (MPE) during the chargedischarge processes of the battery, thus it can provide information on the ionic and electronic transport simultaneously, making it a powerful tool to clarify the charge storage mechanism of novel electrode materials. For example, EQCM was successfully applied to investigate the charge-discharge processes of LiMn₂O₄, Li₄Ti₅O₁₂, Sn, Si, Prussian blue, Li-rich oxides, sulfur, organic polymers etc. as anode or cathode materials for batteries. 16,21-25 The charge storage mechanisms of electrode materials include insertion/extraction, alloying/dealloying, etc. For some composite materials, such as C-S@ polyaniline and Li-rich oxides (considered as a composite of Li₂MnO₃ and LiMO₂ (M = Ni, Mn, Co, etc.)), EQCM can also clarify the role of the components in these electrodes. 19,26,27

Uchida and co-workers were the first to monitor the Li+ insertion/extraction process of LiMn₂O₄ at different temperatures and in different electrolytes. 21 The processes of Li insertion/extraction to the spinel LiMn2O4 could be clarified by measuring the mass change during the cyclic voltammetric scanning and galvanostatic charge-discharge. In addition, in LiPF₆/propylene carbonate-ethylene carbonate (LiPF₆/PC-EC) electrolyte, formation of the passivation layer and the dissolution of manganese oxides were also observed via EQCM. Serizawa et al. employed EQCM to reveal the Li⁺ insertion/ extraction process in a Li₄Ti₅O₁₂ (LTO) anode in a LiPF₆/EC/ DMC (dimethyl carbonate) electrolyte.²² In situ monitoring of the mass change of the LTO electrode can be quantitatively achieved during the charging and discharging processes, because the LTO possesses "zero-strain" properties during Li⁺ insertion and low reactivity with an electrolyte. Yagi et al. employed EQCM to analyze the redox behavior of the Prussian blue (PB) cathode in the LiPF₆/EC/DMC electrolyte.²³ By analyzing the quantitative results, they revealed that the adsorption and desorption of PF₆ ions occurred beginning with the redox reactions of PB along with the insertion/extraction of Li⁺ ions (Fig. 5). The extraction of Li⁺ ions followed the adsorption of the PF₆⁻ ions during the PB oxidation process, and further extraction of Li⁺ ions was slowed down. Whereas, the adsorbed PF₆⁻ ions did not affect the insertion of the Li⁺ ions, because the

During anodic sweep (oxidation) Adsorption of PF, ions Extraction of Li+ ions above 3.1 V vs. Li/Li above 3.5 V vs. Li/Li Adsorbed PF₆ ions hinder the extraction of Litions Li+ ion During cathodic sweep (reduction) Desorption of PF₆⁻ ions below 3.1 V vs. Li/Li⁺ Insertion of Li+ ions below 2.8 V vs. Li/Li

Fig. 5 Schematic diagram of the redox behavior of Prussian blue film in 1 M LiPF₆/EC/DMC measured using EQCM. Reproduced from ref. 23 with permission from Royal Society of Chemistry, Copyright 2014.

PF₆⁻ ions desorbed before the insertion of the Li⁺ ions during the reduction of PB. Lutkenhaus and co-workers adopted EQCM to demonstrate a quantitative view of operando ion transport in the poly(2,2,6,6-tetramethylpiperidinyloxy-4-yl) (PTMA) polymer cathode for LIBs. A dual doping process involving Li⁺ expulsion and anion uptake was revealed for the first time.⁵⁹ Yao et al. used EQCM to explore the chargedischarge mechanism of the poly(benzoquinonyl sulfide) (PBQS) polymer electrode for aqueous Zn-ion batteries. Zn²⁺ was found to be the cation species stored in the PBQS polymer with no obvious hydration.⁵⁶

For electrode materials with a large interstitial space in the crystal structure (e.g., graphite, Prussian blue, etc.), anions and solvent in the electrolyte can co-intercalate into the electrodes with metal cations (e.g., Li⁺, Na⁺, Mg²⁺, etc.). Co-intercalation of anions (e.g., PF₆-, etc.) and cations even leads to the development of dual-ion batteries.²⁴ However, the storage mechanisms for metal cations and anions in different solvents have not been well understood yet. Metal ions and anions have different coordination properties in different solvents, leading to distinct mass transport behaviors during the insertion/de-insertion processes. The high sensitivity of EQCM for mass measurement is utilized to investigate the co-intercalation behaviors of metal cations/anions/solvents in batteries. Seidl et al. studied the reversible intercalation of solvated Na-ions into graphite by using EQCM and in situ XRD. 16 Linear ethylene glycol dimethyl ether homologues ("glymes") G_x with x + 1 O-atoms were used as the solvents, where x was in the range of 1–4, as shown in Fig. 6a. It was found that Na-ions together with a solvation shell as a $\operatorname{Na}^+(G_x)_v$ -solvated complex co-intercalated into the graphite forming a transitional stage-2 ternary Na-graphite intercalation compound (GIC), which was followed by a phase transformation to a stage-1 Na-GIC (Fig. 6b). However, it was noteworthy that the G3 system with the co-intercalation of undercoordinated Na⁺(G₃)₁-solvated complexes led to different electrochemistry and slow diffusion, because it formed a transitional stage-2 Na-GIC, which further transformed into a fully sodiated stage-1 Na-GIC with a different stoichiometry of NaC₃₀ (Fig. 6b). Jimenez et al. discovered the reversible PF₆ insertion/de-insertion processes in n-doped polyaniline cathodes in LiPF₆/EC/DMC solution by EQCM (Fig. 6c).²⁴ In addition, the de-insertion of PF₆⁻ anions and the incorporation of solvent molecules inside the polymer film occurred concurrently during the reduction of the electrode (Fig. 6c). The high reversibility of both redox and mass transfer processes in the applied potential window proved this material to be a promising cathode candidate for Li-ion batteries.

The details of alloying/de-alloying processes with Li⁺ in anode materials like Si, Sn, etc. can also be tracked using the highly sensitive EQCM. Li et al. investigated the chargedischarge processes of the Sn anode by EQCM and in situ FTIR.²⁵ The MPE measured by EQCM changed as a function of the applied potential in a cycle. The values were smaller than the theoretical ones during the process of electrolyte decomposition (mainly SEI formation), whereas they were higher than the theoretical values in the alloying/dealloying processes.

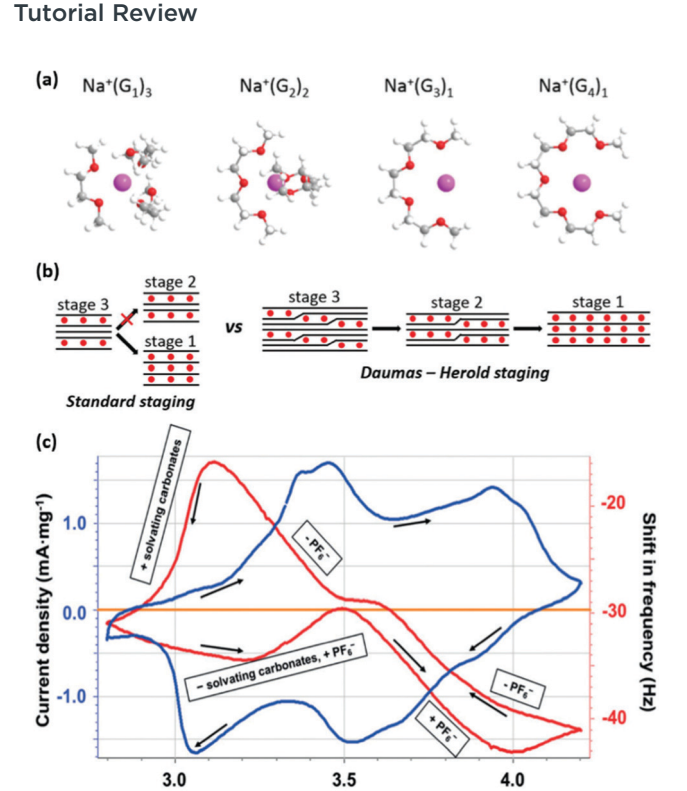


Fig. 6 (a) Ball-and-stick models of $Na^+(G_x)_y$ complexes from different solvents (pink: Na+; red: O-atom; grey: C-atom; and white: H-atom). (b) Different staging models of intercalation of solvated Na⁺ into graphite. Reproduced from ref. 16 with permission from Royal Society of Chemistry, Copyright 2017. (c) EQCM studies of PF₆⁻ anion insertion/de-insertion in lithium n-doped polyaniline cathode. Reproduced from ref. 24 with permission from Wiley. VCH, Copyright 2017.

Potential vs. Li+/Li (V)

Combined with in situ FTIR experiments, EQCM proved that the difference between the theoretical and the experimental MPE values could result from the solvation/desolvation of Li⁺, which was in-turn induced by the alloying/dealloying of lithium with Sn. Ryu et al. explored the electrochemical behaviors of the Si anode in the LiPF₆/EC/DEC (DEC: diethyl carbonate) electrolyte by EQCM, focusing on the irreversible reactions during the first cycle of Li⁺ insertion/extraction.²⁸ In conjunction with FTIR, the results ascribed the irreversible capacity to the reduction of native oxide SiOx and the side reactions involving the electrolyte.

Degradation of the electrodes during cycling is a major cause of the performance fading in a battery. To improve the cycle life of batteries, one strategy is to fabricate composite electrodes for improved electrode stability. 1,29 The chargedischarge processes of composite electrodes are more complicated than simple electrodes, and elucidation of the charge-discharge mechanism in such composite electrodes becomes more difficult. EQCM continues to be capable in the study of the charge storage mechanism of some composite electrodes for batteries. For instance, the shuttling effect of the polysulfide hinders the commercial applications of Li-S batteries; thus, preparing sulfur-based composite cathodes is an effective approach to suppress the shuttling of soluble

lithium polysulfides (LiPS). EQCM was adopted to explore the charge-discharge processes of such sulfur-based composite cathodes. Su et al. investigated the lithium polysulfide sequestration by the polymeric binders in Li-S battery composite cathodes (Fig. 7a).²⁶ EQCM was used to measure the in situ mass change of the sulfur cathodes with polyvinylpyrrolidone (PVP) and poly(diallyldimethylammonium triflate) (PDAT) binders during the charge-discharge processes. The results demonstrated a significantly higher mass gain with the PDAT binder under identical conditions, suggesting that the polycations can effectively adsorb lithium polysulfides via Coulombic attraction between the positively charged backbone and the polysulfide anions. Singh et al. designed a sandwich structure with polyoxometalate $[WZn_3(H_2O)_2(ZnW_9O_{34})_2]^{12-}$ (ZnPOM) in a poly(1-vinyl-3(2-(2-methoxyethoxy)ethyl)imidazolium) (PVIMo) matrix as a composite cathode to improve the performance of Li-S batteries.²⁷ EQCM studies suggested that ZnPOM facilitated fast oxidation of LiPS to elemental sulfur (Fig. 7b), which in turn reduced the LiPS shuttling. The loss of sulfur was negligible even after 120 cycles of charge-discharge, as further confirmed by EQCM.

As a composite of layered Li₂MnO₃ and LiMO₂ (M = transition metals), Li-rich cathodes deliver high capacity in Li-ion batteries. However, the origin of their high capacity in the first cycle is still in controversy. Yin et al. comparatively studied the first-cycle behavior of $x \text{Li}_2 \text{MnO}_3 \cdot (1 - x) \text{LiNi}_{0.3} \text{Co}_{0.3} \text{Mn}_{0.4} \text{O}_2$ (x = 0, 0.5, 1) cathode materials by using EQCM (Fig. 7c). 19 By combining the results of mass change, MPE analysis and in situ EIS, they showed that the activation process of Li_{1.2}Ni_{0.12}Co_{0.12}Mn_{0.56}O₂ (0.5Li₂MnO₃·0.5LiNi_{0.3}-Co_{0.3}Mn_{0.4}O₂) was facilitated by the synergistic effect between the layered Li₂MnO₃ and LiNi_{0.3}Co_{0.3}Mn_{0.4}O₂ structures, which generates an extra-high capacity. In addition, it was also found that the activation of Li2MnO3 in Li-rich materials was governed by the electrochemical decomposition (oxygen redox), whereas chemical decomposition (Li₂O evolution) dominated for bare Li₂MnO₃ activation.

5.1.2 Electrode structural evolution. Repetitive ion insertion/de-insertion during the charge-discharge processes can induce substantial structural changes in the electrodes, causing phase transformation, evolution of surface morphology (e.g., change in roughness), change of volume (i.e., strain), change in mechanical properties, etc. 11 EQCM-D, as a unique probe for hydrodynamic and viscoelastic properties of different electrode configurations, can be used to detect these structural evolutions.

Levi, Aurbach, and co-workers employed the hydrodynamic model to track the in situ ion insertion of LiFePO4 in aqueous solutions,9 and the intercalation-induced phase transitions of LiFePO₄ (Fig. 8a). 12 They found that Li⁺ had a higher tendency of insertion into FePO₄ over Na⁺ in a mixed aqueous solution of Li₂SO₄ and Na₂SO₄ (Fig. 8c). The dynamic mechanical response of the Li_xFePO₄ host to the guest ion (Na⁺ vs. Li⁺) insertion have been studied qualitatively, indicating a nonuniform deformation of the FePO₄ electrode. Using a microarray of composite Li_xFePO₄ electrodes, a significant asymmetry between the charge and discharge behaviors of

(b) (a) Polycation Binder 500 Cell Potential ۸i 0.16 CF₂SO₂ 400 0.08 300 Ņ Li₂S_x Adsorption 200 0.00 CH₃ i (mA) 100 -0.08 -0.16 -100 -200 -0.24**Conventional Binder** 300 2.6 2.0 2.4 State of Lithiation E (V vs. Li/Li*) (c) mpe = -12.65Flectrode materials Li₂MnO₃ activation mpe = -7.0in Li-rich oxides Quartz crystal U∇ mpe = -1.51Potential Δf Pure Li₂MnO₃ activation Normal Li⁺ extraction

Fig. 7 Schematic illustrations of EQCM revealing the charge storage mechanisms of some composite electrodes. (a) Sulfur cathodes with polycation binders. Reproduced from ref. 26 with permission from American Chemical Society, Copyright 2017. (b) PVIMo–ZnPOM/C/S composite. Reproduced from ref. 27 with permission from Royal Society of Chemistry, Copyright 2019. (c) Li₂MnO₃ and Li-rich cathodes. Reproduced from ref. 19 with permission from American Chemical Society, Copyright 2019.

Li_xFePO₄ electrodes was observed, and it presumably originated from a broad particle size distribution of the active material. The fraction of particles experiencing phase transformation was calculated and directly compared with the changes in the effective thickness and permeability length of the active material film. Dimensional variations of the thin active film generated from different molar portions of the pristine and transformed phases gave rise to non-uniform deformations of the intercalated particles. Their research confirmed the collective intercalation behaviors of LixFePO4 particles during the electrochemically caused phase transition process. Levi and co-workers further introduced a new comprehensive methodology based on multi-harmonical EQCM-D measurements, followed by hydrodynamic EQCA modelling.⁴ The newly developed in situ EQCM-D successfully provided the information of intercalation-induced changes of the porous LiMn₂O₄ electrode at the mesoscopic scale in batteries (Fig. 8d). The results showed that an initially completely lithiated LiMn₂O₄ particle, which had a characteristic size of 200 nm, shrank when de-intercalated, as a consequence of the unit cell volume decreasing.

The successful applications of EQCM-D in battery research attract more interest, particularly for *in situ* study of the change in the structure of electrode materials. Shpigel *et al.* conducted EQCM-D to monitor the gravimetric and viscoelastic changes of Ti₃C₂(OH)₂ (MXene) electrode materials during the Li⁺

insertion/extraction processes in aqueous Li2SO4 solutions (Fig. 8b). 14 There was always one water molecule accompanying each Li⁺ intercalating into MXene. Based on EQCM-D monitoring and advanced viscoelastic modeling (extended Voight-type model), solvent-dependent viscoelastic changes and periodic stiffening/softening upon fully reversible Li⁺ insertion/ deinsertion into an MXene electrode were revealed to contribute to the excellent cycling performance (Fig. 8e). Shpigel et al. also used EQCM-D to determine a new strain-accommodation mechanism in NaFePO₄/PVdF electrodes with high-strain, via relaxation of the binder network surrounding the intercalated particles. 10 The mechanical degradation of the polymer network completely occurred (in a hard and tough manner) during long-term cycling of NaFePO₄ electrodes in aqueous solutions. In contrast, in aprotic solutions, a softened binder easily accommodated the high transformation strain (a soft and tough behavior), ensuring excellent cycling performance of the electrode.

Charge

5.1.3 Electrochemical synthesis by ion-exchange. Battery materials can be synthesized using an electrochemical route (e.g., ion-exchange), which can regulate the structure at the molecular level. Being highly sensitive and precise, EQCM can be used to monitor the electrochemical synthesis processes. Sevinc *et al.* reported the *in situ* EQCM observation of the formation of pure olivine NaFePO₄ from chemically synthesized LiFePO₄ nanoparticles via an electrochemical ion-exchange

Tutorial Review Chem Soc Rev (b) (a) Solution bulk H_iO 🥠

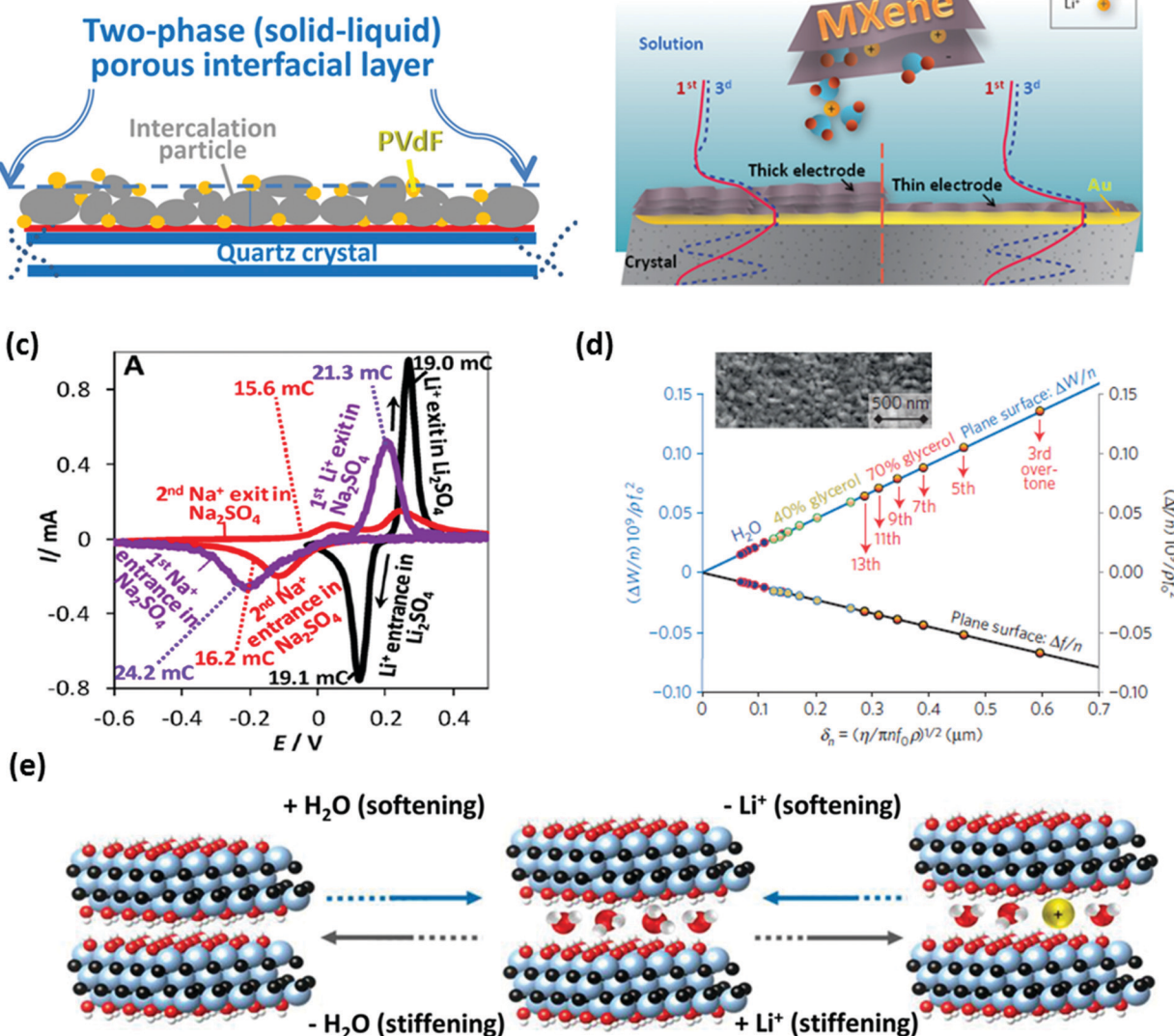


Fig. 8 EQCM-D studies of changes in structure. (a) Collective phase transition dynamics in microarray composite Li_xFePO₄. Reproduced from ref. 12 with permission from American Chemical Society, Copyright 2013. (b) Scheme showing EQCM-D study of MXene electrodes. Reproduced from ref. 14 with permission from American Chemical Society, Copyright 2017. (c) CV curve for Li_xFePO₄ in different solutions. Reproduced from ref. 9 with permission from American Chemical Society, Copyright 2013. (d) Hydrodynamic spectroscopic characterization of an ideally flat Au-coated electrode surface. Reproduced from ref. 4 with permission from Springer Nature, Copyright 2015. (e) Li-ion insertion/extraction-induced viscoelastic changes in MXene electrodes. Reproduced from ref. 14 with permission from American Chemical Society, Copyright 2017.

route. 30 First, the LiFePO₄ nanoparticles were electrochemically delithiated and converted to FePO₄ in a 1 M Li₂SO₄ electrolyte. Then, FePO₄ was further inserted by the Na-ions in a Na₂SO₄ electrolyte with the same electrochemical method to produce NaFePO₄ nanoparticles. The electro-gravimetric data validated the Li/Na ion exchange processes and the formation of NaFePO₄. The phase transformation of LiFePO₄ to NaFePO₄ was proved by in situ XRD during the charge-discharge processes. The as-prepared NaFePO4 was used as a cathode for aqueous Na-ion/polysulfide batteries, and achieved excellent performance.

In summary, in this section, we discussed three categories of EQCM studies related to the ion insertion/de-insertion

behaviors in battery electrodes, including charge storage mechanism, evolution of structural properties and electrochemical synthesis by ion-exchange. The unique advantages of EQCM enable in-depth investigations on the charge storage mechanism of emerging novel electrodes (e.g., Prussian blue, Li-rich oxides, C/S composite, etc.) and co-intercalation behaviors. The transition state of battery electrodes through different charge storage mechanisms (e.g., intercalation-type, alloying-type, etc.) can be monitored in situ. In addition, the effects of individual components on the properties of composite electrodes (e.g., C/S, TiO₂/PEDOT, Li₂MnO₃/LiMO₂, etc.) and the impact of solvents on the co-intercalation processes can be clarified. Furthermore, EQCM can also validate the

Chem Soc Rev **Tutorial Review**

detailed ion-exchange processes during electrochemical synthesis. The advanced EQCM-D technique, which serves as a hydrodynamic and viscoelastic probe for different electrode configurations, has been adopted to obtain a better understanding on the evolution of the structure induced by ion insertion/deinsertion, e.g., phase transformation, viscoelastic changes, volume-change related stress, etc.

5.2 Nucleation derived from electrolytes

5.2.1 Ion electrodeposition on alkali metal anodes. Alkali metals (e.g., Li, Na, etc.) are desirable anode materials for future batteries, due to their high theoretical specific capacity and low reduction potential. Nevertheless, practical application of pure alkali metal anodes remains a distant objective, mainly due to the dendrite formation at the anode surface which leads to poor performance (low coulombic efficiency, poor cycling stability, etc.) and failure by short circuiting.29 In some alkali metal batteries, such as Li/Na-S, Li/Na-air, etc., forming a robust SEI layer on the alkali metal surface is an effective remedy to suppress the dendrite formation. Understanding the metal electrodeposition processes (e.g., the effect of potential, lithium salt anions, additives in the electrolyte, HF impurities, evolution of the electrolyte during deposition, etc.) is essential to construct stable metal anodes. The non-damaging EQCM technique, which has been widely used to investigate metal (Ni, Cu, Zn, etc.) plating and corrosion, is also a capable tool to study the electrodeposition processes of alkali metal in batteries.^{6,11}

Aurbach reported the earliest EQCM study on lithium deposition/dissolution.31 Based on three sets of calculations on these parameters: (1) the actual MPE values for Li deposition-dissolution stages and their evolutions during each stage (along with distinctive time domains), (2) the Coulombic efficiency for the repeated Li anode charge-discharge cycling, and (3) the mass equilibrium per cycle during repeated Li deposition-stripping cycling, they examined several electrolytes to find suitable systems for Li metal batteries. Among the analyzed solutions, they identified that in the 1,3-dioxolane/ LiAsF₆ solution the Li cycling efficiency was close to 100% and the MPE values for both deposition/dissolution steps were 7, an ideal case for Li metal cells. In this electrolyte, the Li electrode was fully passivated and lithium deposition was highly uniform. By contrast, the lithium electrodes in EC-DMC and EC-THF (tetrahydrofuran) exhibited poor performance because of the pronounced reactions between the deposited Li and the solution species. These reactions resulted in non-uniform dendritic Li deposition, which repeatedly exposed fresh lithium to the solution without effective passivation at the surface.

The type of lithium salt, electrolyte additive, and impurities (e.g., HF) generated from the side-reactions can all affect the electrodeposition process, due to the different chemical environment around the ions and the different side reactions. Smaran et al. employed EQCM to study the initial stage of the lithium deposition/dissolution using three kinds of electrolyte salts including LiPF₆, lithium bis(trifluoromethane sulfonimide) (LiTFSI), and lithium bis(fluorosulfon)imide (LiFSI) in tetraglyme (G4) (Fig. 9a).³² Based on the obtained MPE values,

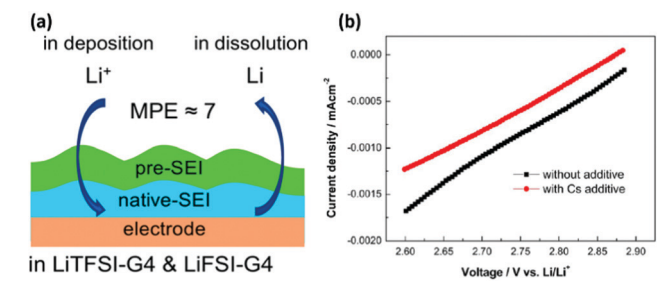


Fig. 9 EQCM studies of the Li deposition behaviors. (a) Scheme showing the typical Li deposition with SEI formation. Reproduced from ref. 32 with permission from American Chemical Society, Copyright 2017. (b) Effect of cesium cation (Cs⁺) additive on the linear sweep voltammetry (LSV) curves of Li deposition. Reproduced from ref. 33 with permission from American Chemical Society, Copyright 2014.

the authors summarized the following three scenarios: (1) MPE \approx 7 (i.e., 5-9): The ideal scenario where only lithium deposition/dissolution took place; (2) MPE \gg 7 (i.e., >9): additional SEI (other than the native SEI) formation and dissolution occurred along with lithium deposition and dissolution; (3) MPE \ll 7 (i.e., <5): during lithium deposition, it was possible that (i) the capacitive charge consumption could not be negligible compared to the charge transfer which led to an increase in Δm , or (ii) lithium deposition led to the formation of massive dendrites. The effect of the SEI layer on lithium deposition/dissolution processes was also discussed. The results showed that additional pre-cycling caused the formation of a "pre-SEI" layer over the "native-SEI" layer in all applied electrolyte solutions. With the pre-SEI present, significant lithium plating/stripping behavior was detected in LiTFSI and LiFSI electrolytes.

Ding et al. used EQCM to explore the effect of a cesium cation (Cs⁺) additive on preventing the growth of Li dendrites (Fig. 9b).³³ It was proposed that Cs⁺ adsorbed but did not deposit on the active sites of the Li electrodes and thus Li was forced to deposit in regions away from the protuberant tips. The mechanism behind such a method to achieve dendrite-free Li deposition was called self-healing electrostatic shield (SHES). A current response in the voltage region of 2.86–2.6 V (vs. Li/Li⁺), in which there was no obvious reaction between the gold electrode and the PC-based electrolyte, was attributed to the capacitive adsorption of cations on the gold electrode surface. An MPE value of 15.86 g mol^{-1} in the electrolyte with Cs^+ was higher than that of 12.22 g mol⁻¹ in the electrolyte without Cs⁺. Considering that Cs⁺ (molar mass is 132.91 g mol⁻¹) was the only cation species other than Li⁺ in this electrolyte which can be adsorbed on the surface of the working electrode, the EQCM results support the SHES mechanism that Cs⁺ cations can adsorb onto the Li electrode during Li deposition.

5.2.2 Nucleation on metal-O2 battery cathodes. As a promising candidate for the next-generation energy storage system, lithium-O2 batteries (mainly non-aqueous aprotic Li-O₂) have attracted wide attention due to their extremely high theoretical energy density (3505 W h kg⁻¹). Li-O₂ batteries differ from traditional Li-ion batteries in that rather than **Tutorial Review** Chem Soc Rev

intercalating Li⁺ ions into a host material, Li⁺ directly reacts with oxygen mainly resulting in the precipitation of Li₂O₂, in addition to other insoluble Li-O2 compounds in non-aqueous media. However, the reaction mechanism of Li-O2 batteries is still in controversy, including disagreements on the specific reaction products during the charge-discharge processes, the stability of the electrolyte, and the types of the generated lithium oxides.34,35 These complicated electrochemical processes and instability issues require careful attention to be paid to every component of the Li-O₂ battery. As an in situ, nondamaging tool, EQCM has been adopted to monitor the electrochemical processes (e.g., lithium oxide formation/evolution, electrolyte stability) during the discharge-charge of Li-O₂ cells, and clarify the specific effects of Li salt-solvent pairs (such as type of solvent, degree of Li⁺ dissociation, Li⁺ concentration, etc.), catalyst, and impurities (e.g., H2O, HF, etc.).

Several groups studied the discharge-charge mechanisms in different electrolytes using EOCM. Torres et al. explored the oxygen reduction reaction (ORR) in LiPF₆/DMSO (DMSO: dimethyl sulfoxide) electrolyte using EQCM during galvanostatic cathodic and anodic pulses, chronoamperometry (CA), and CV experiments. 38 The mass of the Li₂O₂ deposited per unit area and the variation of shear wave energy losses (ΔR) depended on the experimental conditions (e.g., type of solvents, specific current, trace water amount, scan rate and time of

deposition). These dependencies were linked to the different ORR mechanisms in a bulk LiPF₆/DMSO electrolyte and at the electrode/electrolyte interface: (i) surface electrochemical/ chemical deposition of Li₂O₂ (solid) and (ii) solution phase disproportion of LiO₂(solution) yielded large Li₂O₂ particles. Galiote et al. combined EQCM and EIS to determine the rate constants for each elementary step of ORR for a platinum electrode in LiClO₄/dimethoxyethane (DME), using a kinetic model in the frequency domain.³⁹ The kinetic constants pointed out that the adsorption energy of oxygen molecules is high; the electrons are transferred slowly to the molecules adsorbed on the platinum sites; and the platinum site is partially blocked due to the formation of reaction products insoluble in organic solvents. Moreover, Li₂O₂ was the preferential product of the reaction during the electrochemical step, thus ensuring more electrons transferred to each oxygen molecule adsorbed onto the platinum sites and higher power and energy capacity of the battery. The results suggested that EQCM can distinguish the ORR from the side reactions induced by the decomposition of solvent and the accumulation of $\text{Li}_x O_2$ (1 $\leq x \leq 2$) adsorbed on the electrode. The reaction rate of the ORR was limited by the electron transfer to the oxygen molecules which were strongly adsorbed on the platinum sites, particularly when the amount of reaction products (Li₂O₂) had already been adsorbed on the electrode.

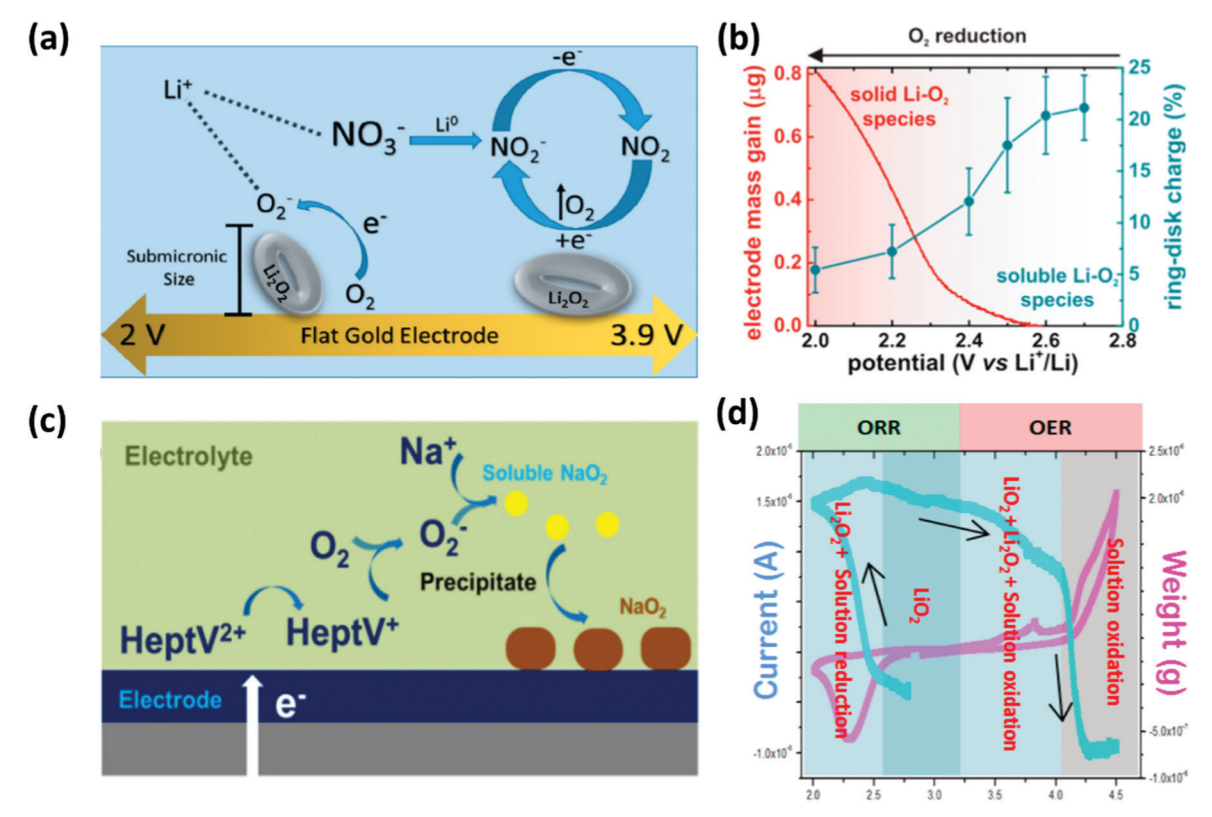


Fig. 10 Nucleation behaviors of $Li(Na) - O_2$ batteries in different electrolytes revealed by EQCM. (a) Growth mechanisms of Li_2O_2 in $LiClO_4$ -based electrolyte. Reproduced from ref. 35 with permission from American Chemical Society, Copyright 2016. (b) Catalytic behavior of LiNO₃. Reproduced from ref. 36 with permission from American Chemical Society, Copyright 2015. (c) Shuttling effect model of the HeptVBr2 on the formation of NaO2. Reproduced from ref. 20 with permission from Elsevier, Copyright 2020. (d) Scheme showing the stability of polar aprotic solvents toward lithium oxides. Reproduced from ref. 37 with permission from American Chemical Society, Copyright 2013.

Effects of specific electrolyte parameters (type of solvent, degree of Li⁺ dissociation, Li⁺ concentration) were discussed in several reports. Kwabi et al. employed EQCM to investigate the effect of solvents (DME and DMSO) on the ORR process in LiClO₄-based electrolyte (Fig. 10a).³⁵ A striking difference between DME and DMSO electrolytes was seen at the beginning of the ORR process. The differences between DME and DMSO were observed in the onset potentials ($-50 \text{ mV } \nu s. -200 \text{ mV}$) at the frequency changes and the ORR current, the frequency change during the reduction (-140 Hz vs. -900 Hz), and the reversibility of the OER (oxygen evolution reaction) (42% vs. 15%). Based on the MPE values calculated in two electrolytes and the RRDE results, a solution-mediated growth mechanism driven by self-assembly and aggregation of solvated Li⁺-O₂species was proposed. In another work, Sharon et al. applied EQCM to comparatively study ORR/OER behaviors in LiNO₃/ diglyme and LiTFSI/diglyme electrolytes (Fig. 10b).36 The voltammetric and gravimetric responses of these EQCM experiments in LiNO₃ solutions were much more pronounced than in LiTFSI solutions. A catalytic behavior of LiNO₃ was uncovered,

Chem Soc Rev

Selection of an appropriate catalyst is crucial for the performance of Li(Na)–O₂ batteries. Rational material design of new catalysts and modification to existing catalysts depends on mechanistic understanding of the reactions. Different catalysts tend to result in different reaction mechanisms in Li(Na)–O₂ batteries. Pan and co-workers employed EQCM to study the effect of a soluble HeptVBr₂ redox catalyst on the formation mechanism of the oxygen reduction product (NaO₂) (Fig. 10c).²⁰ The MPE value in the system without a redox mediator was 56.4 g mol⁻¹, while it decreased to 29.4 g mol⁻¹ when a redox mediator was present. Combined with *in situ* AFM and laser particle size measurement, EQCM revealed a shutting effect offered by the redox mediator. The electrons could be shuttled to the electrolyte *via* the redox mediator, enabling the

indicating that LiNO₃ can serve as an electrolyte and redox

mediator to improve both the ORR and OER performance.

formation of NaO₂ in the bulk of the solutions, rather than within the limited region on the surface of the electrode. Torres et al. used EQCM and RRDE to reveal the role of the soluble iron(II) phthalocyanine (FePc) catalyst in the ORR mechanism. Without FePc, the shear wave dissipation was negligible and the mass deposited was less than that observed with the redox shuttle FePc. 40 With soluble FePc in the electrolyte, the EQCM result showed a MPE value close to 23 g mol⁻¹ for the formation of Li₂O₂ at low current densities, and a larger MPE value at higher current densities, probably due to the solvent codeposition or the trapped DMSO in the surface deposit. The formation of Li₂O₂ was verified by RRDE. The effect of the concentration of FePc on the current, mass, and shear wave dissipation response were also investigated. The EQCM and RRDE results confirmed that the FePc shuttle favored the solution phase mechanism during the ORR by one-electron reaction with further formation of insoluble Li₂O₂ at the electrode surface.

The stability of the electrolyte, especially toward lithium oxides, is vital to determine whether such an electrolyte is suitable for Li-O2 batteries. The mediators generated in situ during the electrolyte decomposition allow the highly sensitive EQCM to evaluate the stability of the electrolyte during the discharge-charge processes. Some ORR products are soluble in the electrolyte as reflected in the current response of electrochemical reactions, without showing pronounced change in the mass of the electrode. Sharon et al. adopted EQCM to investigate the side reactions in Li-O2 battery systems using 1 M triglyme/LiTFSI (bis-(trifluoromethanesulfonyl)imide) electrolyte, which is a typical polyether solution (Fig. 10d).³⁷ The ideal MPE values for LiO2 and Li2O2 formation at the O2 cathode were 39 and 23 g mol⁻¹, respectively. The ideal MPE value for mutual transformation between LiO_2 and Li_2O_2 was 7 g mol⁻¹. A mechanism was proposed based on the calculated MPE values, and it was further confirmed by additional analysis using FTIR, NMR and matrix-assisted laser desorption/ionization (MALDI). During the ORR, the reactions of the oxide

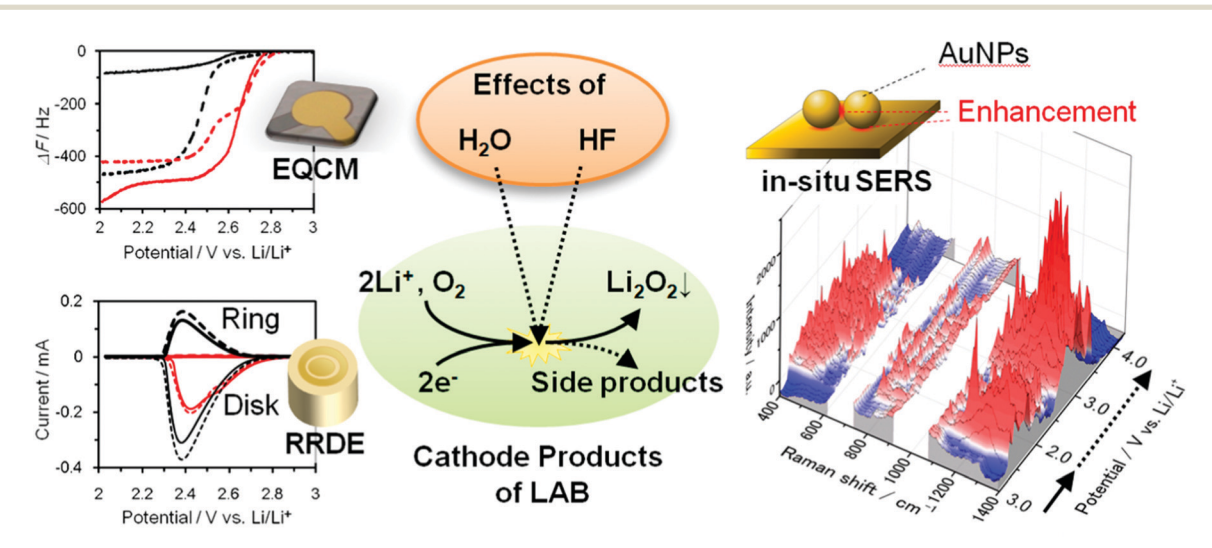


Fig. 11 Combination of EQCM with RRDE, in situ SERS to reveal the effect of water, HF on the distribution of discharge products at the $Li-O_2$ battery cathode. Reproduced from ref. 17 with permission from American Chemical Society, Copyright 2018.

Tutorial Review Chem Soc Rev

moieties with the solution species impeded the sequential reduction of ${\rm LiO_2}$ and ${\rm Li_2O_2}$. Thus, by analyzing the OER process, it was shown that the products which formed at the ORR stage were all oxidized and disappeared from the electrode. Degradation of ${\rm Li_2O_2}$ was also mixed with side reactions including oxidation of the solution species. The presented mechanism above is helpful to find solutions for the protection of ether solvents.

The electrolyte for the Li-O2 battery always contains impurities, which mainly include HF and H2O. The effect of such impurities on the charge-discharge processes of the Li-O₂ batteries needs to be clarified. Tomita et al. combined EQCM, RRDE, and in situ Raman to explore the effect of HF and H₂O on the potential-dependent product distribution on the gold electrode in DMSO solutions (Fig. 11).17 The results revealed that the potential-dependent reaction products were affected by impurities even a small amount, and therefore the cathode reaction mechanisms of the Li-O2 battery were changed. In a relatively positive potential range, soluble products such as O₂ and LiO2 were dominant in HF-free solutions, while "insoluble" LiO₂ and LiF deposits are the major products in HFcontaining solutions. For the more negative potential range, insolvable, LiO2 was transformed to the Li2O2 via either disproportionation reaction or electrochemical reduction. Li₂O formed at a much more negative potential region. H2O in the solution not only transformed Li₂O₂ to LiOH but also induced side reactions causing the formation of H2O2 and LiOOH, which subsequently led to the DMSO decomposition.

6. Interfacial reaction and reconstruction mechanisms

6.1 Interphasial formation/evolution

Due to the big difference in the physicochemical properties between the electrode materials and the electrolyte, and the intense electric field at the electrode/electrolyte interface, reactions at the interface result in the formation of interphase(s). The electrode/electrolyte interphase (solid electrolyte interphase (SEI) for anodes, cathode electrolyte interphase (CEI) for cathodes) play a vital role in the electrochemical performance of batteries. 41 An ideal electrode/electrolyte interphase is a stable, passivating, and protecting layer with a high ionconductivity and enough mechanical stability. In addition, it can prevent further electrolyte degradation by blocking the electron transport through the interface, while simultaneously allowing alkali metal ions to diffuse through. An electrode/ electrolyte interphase can also accommodate the volume change of the electrode, minimize exfoliation of the active material, and delay performance degradation during chargedischarge. 41 The physicochemical properties of the electrode/ electrolyte interphase are determined by the formation process. However, the mechanism behind the formation of interphases is still controversial. This section summarizes the application of EQCM techniques to study different aspects of SEI/CEI layers in battery electrodes, including the characterization of the SEI/CEI formation process and the effects of the electrode, the type of the electrolyte, and additives.

6.1.1 Formation/evolution of interphases on inert electrodes. One way to study the mechanism of interphasial formation/evolution is using an inert metal as a working electrode. Some metals (*e.g.*, Pt, Au, *etc.*) are only electrochemically active under very low voltage (<0.5 V vs. Li/Li⁺), and some (*e.g.*, Ni and Cu) are inherently inactive in the battery system. Inert electrodes can eliminate the interferences from the lithiation–delithiation processes of an active material and the effects of the conducting agent and binder. Such inert electrodes are suitable to individually study the effect of applied potential on the mechanism of interphasial formation/evolution in a wide voltage range. The decomposition of electrolytes at low voltages (reduction) and high voltages (oxidation) are the two important parts of the interphasial formation reactions, which were explored by many researchers using EQCM.

Aurbach et al. reported the earliest EQCM study of interphasial formation in 1995. They analyzed the formation process of a surface film induced by electrolyte reduction on the Au electrode in propylene carbonate (PC) solutions. 42 EQCM was proposed as a tool for determining the molecular weight of the species precipitated on the electrode surface. In non-aqueous LiAsF₆/PC solutions, solvent reduction was dominant and ROCO₂Li was formed (R is an organic group) at potentials lower than 1 V, while the salt anion reduction became dominant at higher potential range and LiF was formed. At the lower potential region, the first layers formed comprised ROCO2Li and Li2CO3, which was owing to the secondary reaction between the trace H₂O and ROCO₂Li. Then, the reduction reactions of salt became dominant since the reduction process which continued through the deposited films was more selective. For the water-containing LiAsF₆/PC electrolytes, the EQCM studies revealed that the hydrated films were formed on the electrode surface, and the mass accumulation was mainly on account of the hydrating water. A mass of hydrating water absorbed on the surface films driven by the potential where these films were formed. With LiPF₆ solutions, the calculated MPE values agreed with the precipitation of LiF and Li_xPF_v or $\text{Li}_x \text{POF}_v$ species when the potential was stepped to 1.5 V (vs. Li/Li⁺). The MPE values calculated for steps to lower potentials agreed with the precipitation of LiF as the major surface species via the reaction between HF and ROCO₂Li.

The formation of SEI is generally caused by the decomposition of the electrolyte, so the properties of the lithium salt and the solvent are important. Combining EQCM with other characterization tools, and influences of different electrolytes on the formation of SEI can be compared and researched systematically. Aurbach and co-workers combined *in situ* EQCM, FTIR, AFM, and EIS to study the surface film formation on nonactive-metal electrodes (Au and Ni) in ethylene carbonate (EC)-based electrolytes. ¹⁸ The electrolytes studied included EC-dimethyl carbonate (EC-DMC) and EC-tetrahydrofuran (EC-THF) mixtures with Li salts including LiAsF₆, LiPF₆, LiClO₄, and LiBr. Among these solution systems, the reduction products of EC were the dominant component in the surface films. Nevertheless, in LiPF₆-containing electrolytes, Li salt reduction products became

dominant in the surface films. Sonoki *et al.* employed EQCM and XPS to investigate the early stage in the formation process of the SEI layer in four electrolyte solutions, including 2.0 mol $\rm L^{-1}$ LiBH₄ in THF, 1.0 mol $\rm L^{-1}$ LiPF₆ in EC–DEC, 1.0 mol $\rm L^{-1}$ LiTFSA (lithium bis(trifluoromethanesulfonyl)amide) in EC–DEC and 1.0 mol $\rm L^{-1}$ LiTFSA in diglyme. ⁴³ According to the EQCM results, the SEI layer formed in the LiBH₄/THF electrolyte was negligible. The initial potential of SEI formation in the LiPF₆ electrolyte was 2.3 V ν s. Li/Li⁺, and continuously grew even at an anodic scanning process. The LiTFSA-containing electrolyte formed an SEI layer around 1.5 V ν s. Li/Li⁺. XPS was used to characterize the specific components of the SEI in different electrolytes at high potentials. The LiPF₆

electrolyte formed a solid LiF layer whereas the LiTFSA electrolyte formed a thick SEI layer containing organic components, including

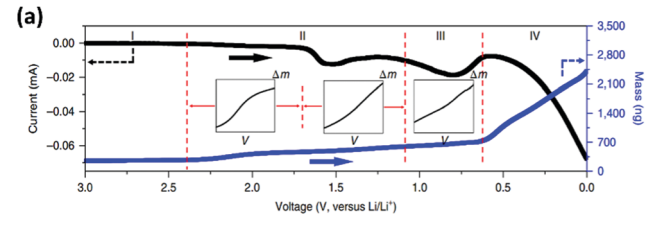
polyether and lithium alkyl carbonate.

Chem Soc Rev

6.1.2 Formation/evolution of interphases on active electrodes. Due to the insertion/de-insertion of metal ions during charge–discharge and the interaction between the electrode and the electrolyte (*e.g.*, the electrode material catalyzes the decompostion of the electrolyte), the formation/evolution of interphases on practical battery electrodes is more complicated than that on inert electrodes. EQCM has been applied to study the formation reactions of interphases on different active electrodes (*i.e.* carbon, Si, Sn, Li₄Ti₅O₁₂, Li-rich, *etc.*), and the viscoelasticity of the interphasial film was quantified *via* EQCM-D.

Pan and co-workers investigated the formation process of SEI on graphitic electrodes.⁵ Based on the in situ EOCM (Fig. 12a), in situ AFM, and DEMS data, LiF (25.9 g mol⁻¹) and lithium alkyl carbonates (80.9 g mol⁻¹ for EC product or 81.9 g mol⁻¹ for DMC product) were identified as the main chemical components at different potentials. They proposed five distinct chemical or electrochemical processes of the SEI formation (Fig. 12b): (1) the formation of LiF at 1.5 V (vs. Li/Li⁺); (2) Li⁺ (solvent)_x co-intercalation at 0.88 V (vs. Li/Li⁺); (3) initial reduction of EC at 0.74 V (vs. Li/Li⁺); (4) major reduction of EC at lower potentials; (5) lithium alkyl carbonates produced by EC reduction are partially re-oxidized during anodic scans above 0.3 V (vs. Li/Li⁺). Moreover, it was revealed that the re-oxidized capability of the SEI depended on the cycling status: newly formed SEI readily disappeared on recharging, but it became more difficult to be oxidized on electrodes after the long cycling process.

EQCM was also applied to characterize the SEI formation reactions on other anode materials, such as Li₄Ti₅O₁₂, Si, Sn, *etc.* Dargel *et al.* employed EQCM-D to study the SEI formation on Li₄Ti₅O₁₂ anode materials in EC-DMC with LiTFSI, LiPF₆, and LiPF₆ + 2% vinylene carbonate solutions. ⁴⁴ EQCM-D was applied to record the resonance frequency and the change in width of the resonance peak of electrodes in an air environment, in contact with Li-battery electrolyte solutions at opencircuit voltage and under an applied potential (Fig. 13a–c). The acoustic multilayer formalism was used to build a self-consistent viscoelastic model of the composite Li₄Ti₅O₁₂ electrodes, in order to transform the EQCM-D measured data to gravimetric and viscoelastic changes, which were caused by the



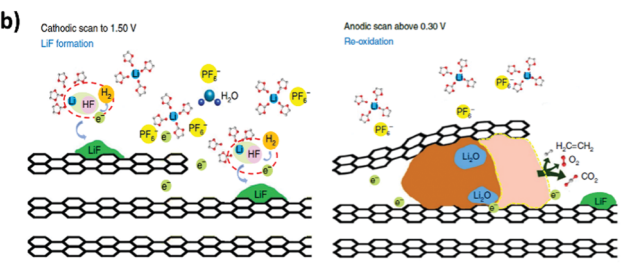


Fig. 12 EQCM studies of interphasial formation/evolution on active electrodes. (a) CV and mass change of graphite, and (b) corresponding schematic illustration of the reaction mechanism. Reproduced from ref. 5 with permission from Springer Nature, Copyright 2018.

formation of SEI. It was revealed that the quality of SEI on the ${\rm Li_4Ti_5O_{12}}$ electrode improved in the sequence of ${\rm LiPF_6} < {\rm LiPF_6} + 2\%$ vinylene carbonate « LiTFSI. Hubaud *et al.* conducted EQCM-D to study the details of the formation and dissolution of SEI on Si anode materials as well as the influence of the ${\rm SiO_2}$ component. During the lithiation process, mass loss was observed for the ${\rm SiO_2}$ -coated Si electrode in both EC/EMC and EC/DEC/FEC (fluoroethylene carbonate) based electrolytes. Combined with NMR measurements, EQCM-D data indicated that the mass loss was caused by the formation and dissolution of ${\rm Li_2O}$.

Compared with the SEI, the CEI formed on the cathode, which originated from electrolyte oxidation, is less distinguished. Benefitting from the high precision, EQCM was applied to study the interfacial chemistry of cathode materials. Yang et al. employed EQCM-D to investigate the formation of a CEI layer on a Li-rich cathode (0.5Li₂MnO₃·0.5LiMn_{0.375}Ni_{0.375}Co_{0.25}O₂) in LiPF₆/EC/EMC electrolyte. 46 It was revealed that the CEI layer formed spontaneously on the electrode surface exposed to the battery electrolyte and the mass of the CEI layer increased as a function of applied voltage. Yin et al. used EQCM to reveal the CEI evolution of layered Li₂MnO₃, LiNi_{0.3}Co_{0.3}Mn_{0.4}O₂, and Li-rich 0.5Li₂MnO₃·0.5 LiNi_{0.3}Co_{0.3}Mn_{0.4}O₂. ¹⁹ The results indicated that the evolution of CEI was highly related to the Li⁺ extraction and insertion process. In addition, the formation of CEI can be well promoted by the changes in the valence of the metal ions (Ni, Co, Mn) in Li-rich

After an age of exploration, carbonate ester-based electrolytes have become the most widely used electrolyte in commercial batteries, due to their overall superior performance. However, carbonate ester electrolytes still suffer continuous decomposition during charge–discharge processes, which affects the cycle life of batteries. ⁴¹Among all the methods to suppress electrolyte decomposition, employing electrolyte additives is one of the most promising, simple, and effective ways. ⁴¹

Tutorial Review Chem Soc Rev

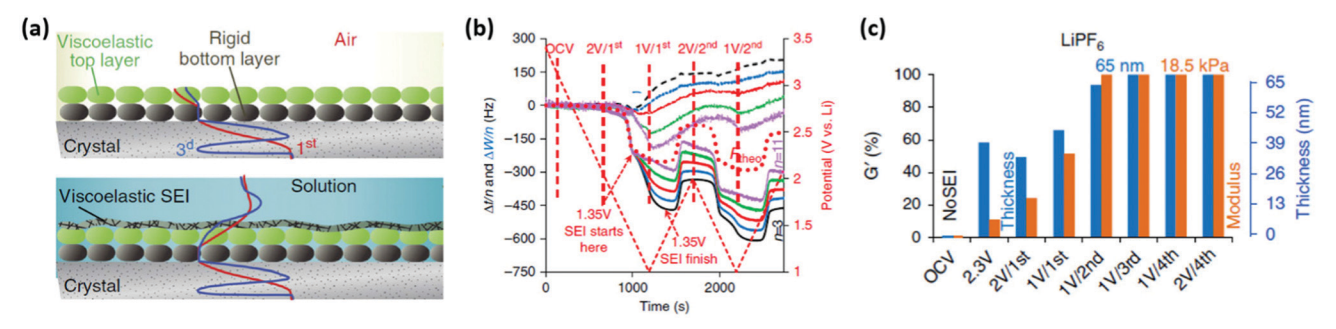


Fig. 13 EQCM-D studies of viscoelastic properties of SEI film. (a) Sketch of velocity profiles for rigid and viscoelastic layers of Li₄Ti₅O₁₂ (LTO) electrodes in air and in electrolyte solution. (b) Frequency and resonance width changes of LTO electrodes at different overtones. (c) Viscoelastic parameters of LTO electrodes when in contact with LiPF₆. Reproduced from ref. 44 with permission from Springer Nature, Copyright 2017.

With the help of EQCM, the influence of different additives on the formation of SEI can be revealed. Yang et al. studied the effect of fluoroethylene carbonate (FEC) additive on the mass and viscoelasticity of the SEI layers on Sn anodes using EQCM-D (Fig. 14a-c). 47,48 Based on the distinctly different CV curves (Fig. 14a) and the frequency changes (Fig. 14c), it was deduced that before Li insertion the initial formation process of SEI was rapid, but varied significantly when the concentration of the FEC additive increased in the electrolyte. By using the Sauerbrey and Voigt viscoelastic models to analyze the EQCM-D data, the behaviors of SEI formation were different when different amounts of FEC additive were added in the electrolyte, which resulted in differences in the estimated mass, shear modulus and viscosity (Fig. 14b). After three cycles, the SEI layer in the pristine electrolyte presented 1.2 times more mass change compared to the film in electrolyte containing FEC additives. In addition, the shear elastic modulus of the SEI layer formed in the presence of FEC was higher than that in the pristine electrolyte at the early stage of lithiation.

6.2 Solid-liquid coordination

The transport of alkali metal ions (Li⁺, Na⁺, K⁺, etc.) at the electrode/electrolyte interface obviously affects the rate performance of the batteries.² Desolvation/solvation behaviors of alkali metal ions alter at the electrode/electrolyte interface with different chemical environments in the bulk electrode

and electrolyte.2 For various electrode/electrolyte systems (factors including electrode type, electrolyte salt, solvent, concentration, etc.), the solid-liquid coordination environment can be quite distinct, resulting in different ionic diffusion routes at the electrode/electrolyte interface and different mass change during the charge-discharge processes. As a molecularlevel mass probe, EQCM can also be applied to study the solid-liquid coordination environment in the batteries.

Pan and co-workers reported a much better rate performance of LiFePO4 in an aqueous electrolyte than in an organic electrolyte. 49 EQCM was adopted to study the mass change of LiFePO₄ in the aqueous and the organic electrolytes respectively. The MPE values in the aqueous electrolyte (12.9/12.6 for oxidation/reduction peak) were higher than those in the organic EC electrolyte (6.7/6.6) (Fig. 15a). A combination with ab initio calculations identified the transient formation of a Janus hydrated interface in the LiFePO₄-H₂O system (Fig. 15b), which eased the Li desolvation process near the surface. Tarascon and co-workers confirmed the solvent-dependent Li⁺ insertion/extraction behavior in LiFePO₄ using EQCM-D.⁵⁰ In an aqueous electrolyte, they proved that Li⁺ desolvated from the water solvation shell near the electrode surface which was different to the orgainc electrolyte. This spatial difference led to a smoother Li⁺ transport across the LiFePO₄-H₂O interface, hence explaning

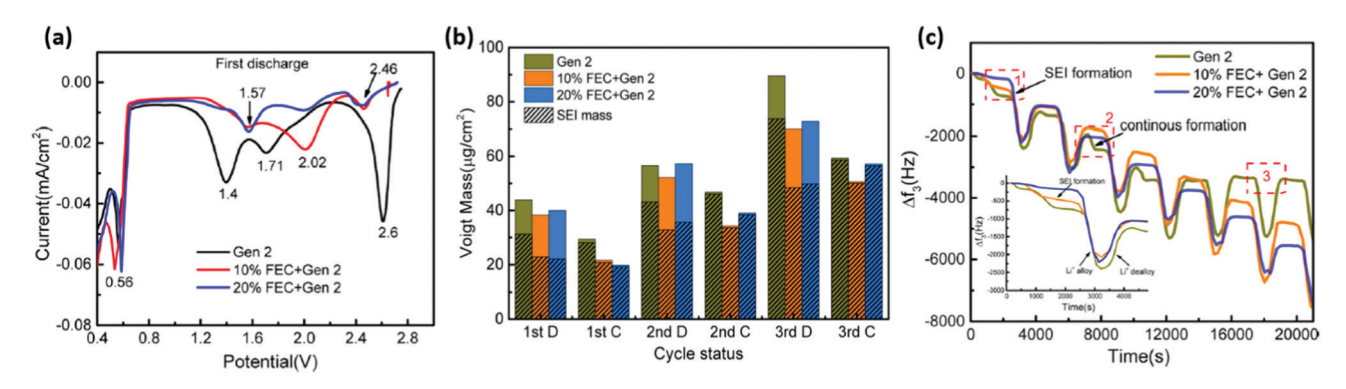


Fig. 14 EQCM studies of the role of electrolyte additives in SEI formation. (a) CV curves, (b) total mass change calculated at the end of each half cycle and (c) representative frequency changes for six cycles of Sn electrode in electrolytes with different amounts of FEC additive. Reproduced from ref. 47 with permission from American Chemical Society, Copyright 2015

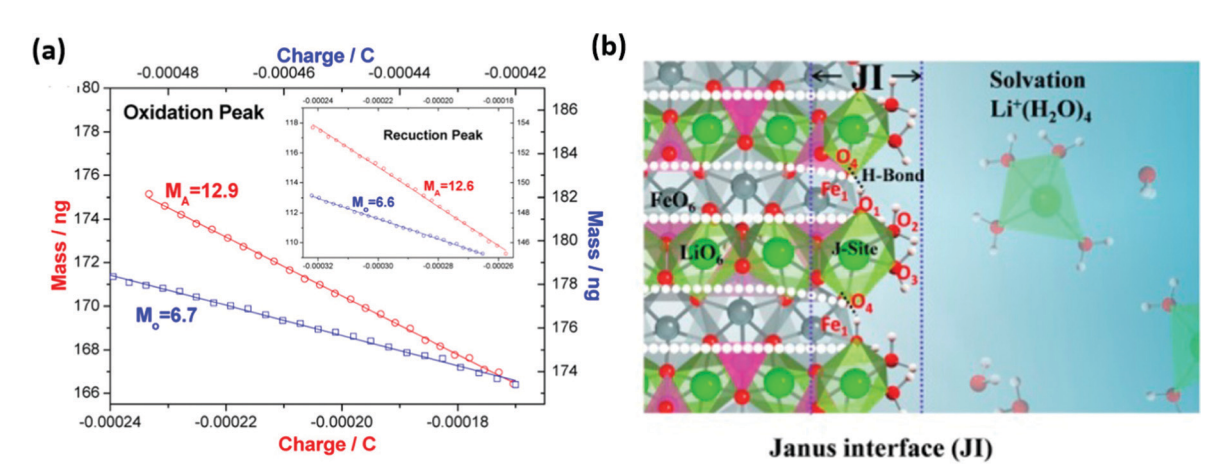


Fig. 15 EQCM studies revealed the solid-liquid coordination at the LiFePO₄/aqueous electrolyte interface. (a) EQCM measured mass change during CV scan of 45 nm LiFePO₄ in aqueous Li₂SO₄ electrolyte. (b) Scheme showing the formation of Janus solid-liquid interface. Reproduced from ref. 49 with permission from American Chemical Society, Copyright 2015.

the difference in the rate capabilities of LiFePO4 in the respective aqueous and organic electrolytes.

A comparative study on the solid-liquid interfacial properties of LiFePO4 (LFP) and NaFePO4 (NFP) was conducted by Pan and co-workers (Fig. 16).8 EQCM demonstrated an anomalous mass change interval around 3.42 V (vs. Li/Li⁺) for LFP nanocrystals in an aqueous eletrolyte (Fig. 16a). Such an abnormal behavior was attributed to the lower redox potential $(\sim 3.31 \text{ V vs. Li/Li}^+)$ at the surface than that $(\sim 3.42 \text{ V vs. Li/Li}^+)$ in the bulk of LiFePO₄ (Fig. 16b and d). While for LFP in the organic electrolyte, and NFP in both aqueous (Fig. 16c) and organic eletrolytes, a normal mass decrease/increase behavior originated from the de-insertion/insertion of Li(Na) ions was observed. For NFP, its surface redox potential was essentially the same as the bulk one.

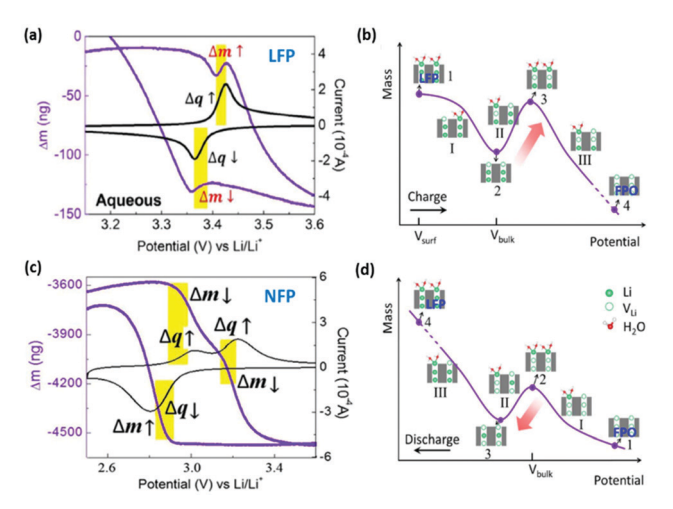


Fig. 16 The mass-potential curve and CV scan measured by EQCM for (a) LiFePO₄ and (c) NaFePO₄ nanocrystals in aqueous electrolytes. The simulated mass-potential curve of the (b) charging, and (d) discharging process for LiFePO₄ in an aqueous system at different stages. Reproduced from ref. 8 with permission from Elsevier, Copyright 2017.

7. Conclusions and prospects

This review systematically summarizes the significant findings in recent battery studies achieved by the advanced EQCM technique. EQCM, which can obtain electrochemical, gravimetric, and beyond gravimetric (e.g., impedance and energy dissipation) information in real time, is a cost-effective and non-destructive characterization method with a simple sample preparation procedure to simulate real-life electrodes. Compared with other techniques for characterizing structure (e.g., XRD, electron microscopy, AFM, etc.) and chemical composition (e.g., FTIR, Raman, EELS, etc.), EQCM bears its own unique advantages, which make it a useful tool for investigation of electrochemical phenomena and mechanisms in batteries.

So far, EQCM has been successfully applied in four main aspects of battery studies, including insertion/deinsertion of ions in electrodes, nucleation of solids from the electrolyte, interphasial formation/evolution, and solid-liquid coordination. It was proved that EQCM is a powerful tool for resolving many unknowns in batteries. In detail, (1) EQCM has been adopted to reveal many controversial mechanisms involving both surface and bulk structure evolution, i.e., the transition state of battery electrodes based on different charge storage mechanisms (e.g., intercalation-type, alloying-type, conversiontype, etc.), co-intercalation behaviors, etc. (2) The non-damaging feature of EQCM makes it unique to detect the intermediates during lithium deposition on anodes, oxygen evolution reaction of metal-O₂ battery and SEI formation/evolution. (3) The molecular-level measurement by EQCM makes it useful for solid-liquid coordination studies. (4) EOCM-D can observe in situ mesoscopic-scale structure changes in practical composite electrodes with a binder.

The current battery studies via EQCM created some new opportunities to deepen the understanding of battery phenomena and pursue high battery performance. Specifically, (1) The present EQCM studies of interphasial formation/evolution on an inert electrode and active battery electrodes indicated a distinct effect of battery electrodes on electrolyte decomposition. (2) EQCM investigations of ion Tutorial Review Chem Soc Rev

electrodeposition on alkali-metal (e.g., Li, Na, K, etc.) anodes can provide clues for finding a solution, e.g., electrolyte optimization, artificial SEI, stable porous host skeletons, etc., to suppress dendrites during charge-discharge. (3) EQCM is a capable tool to study the solid-liquid coordination environment and the charge transfer process at the interface or in the bulk of some novel electrode/ electrolyte systems, e.g., the LiCoO2 cathode in high-concentration EC-based or aqueous electrolyte. (4) EQCM can be used to quantitatively monitor both the electro-synthesis (e.g., ion exchange, electrodeposition, etc.) and charge-discharge processes of some binder-free electrodes, to achieve precisely controlled synthesis for high performance materials. (5) Some novel charge methods such as pulse current were introduced into charging batteries to improve the safety and cycling stability, while the inherent mechanisms are unclear. EQCM can be coupled with such pulse current methods to uncover its role in constructing a stable SEI film, inhibiting the growth of lithium dendrites, etc.

Although previous reports have demonstrated many successful cases, challenges still remain in EQCM studies of batteries. First, despite the extraordinary advantages of EQCM, there is a limitation of EQCM that it cannot provide direct structural and chemical composition information. The current combinations of EQCM with other in situ characterization methods (e.g., XRD, DEMS, FTIR, etc.) cannot evaluate one same system at the same time. Simultaneous techniques such as EQCM-MS are called for. Second, to date, most researchers only used EQCM as a gravimetric tool in a solid/liquid system. However, for many complicated systems, the application of the gravimetric Sauerbrey equation should be done carefully. The current theoretical and experimental recognition of the EQCM-D technique, which can be applied in more complicated systems than gravimetric EQCM, is still insufficient. More attention should be paid to the modeling of battery studies by EQCM-D.

Overall, there is no doubt that EQCM benefits the investigations of the battery phenomena and mechanisms, and new findings continue to inspire the design and optimization of battery components. We believe that this review and perspective will offer an overview of battery studies using EQCM as a key tool, and stimulate new ideas for researchers in further phenomena and mechanisms analysis and developing the next-generation batteries.

Conflicts of interest

The authors declare no conflict of interest.

Acknowledgements

This work was supported by the National Key R&D Program of China (2016YFB0700600 and 2020YFB0704500), Shenzhen Science and Technology Research Grants (no. JCYJ20200109140416788), the Chemistry and Chemical Engineering Guangdong Laboratory (Grant No. 1922018) and China Postdoctoral Science Foundation (No. 2020M680198).

Notes and references

- L. Yang, K. Yang, J. Zheng, K. Xu, K. Amine and F. Pan, Chem. Soc. Rev., 2020, 49, 4667–4680.
- 2 A. M. Tripathi, W. N. Su and B. J. Hwang, *Chem. Soc. Rev.*, 2018, 47, 736–851.
- 3 J. Lu, T. P. Wu and K. Amine, Nat. Energy, 2017, 2, 17011.
- 4 N. Shpigel, M. D. Levi, S. Sigalov, O. Girshevitz, D. Aurbach, L. Daikhin, P. Pikma, M. Marandi, A. Janes, E. Lust, N. Jackel and V. Presser, *Nat. Mater.*, 2016, 15, 570–575.
- 5 T. Liu, L. Lin, X. Bi, L. Tian, K. Yang, J. Liu, M. Li, Z. Chen, J. Lu, K. Amine, K. Xu and F. Pan, *Nat. Nanotechnol.*, 2019, 14, 50–56.
- 6 D. A. Buttry and M. D. Ward, Chem. Rev., 1992, 92, 1355–1379.
- 7 G. Z. Sauerbrey, Z. Phys., 1959, 155, 206-222.
- 8 X. Song, T. Liu, J. Amine, Y. Duan, J. Zheng, Y. Lin and F. Pan, *Nano Energy*, 2017, 37, 90–97.
- 9 M. D. Levi, S. Sigalov, G. Salitra, R. Elazari, D. Aurbach, L. Daikhin and V. Presser, *J. Phys. Chem. C*, 2013, **117**, 1247–1256.
- 10 N. Shpigel, S. Sigalov, M. D. Levi, T. Mathis, L. Daikhin, A. Janes, E. Lust, Y. Gogotsi and D. Aurbach, *Joule*, 2018, 2, 988–1003.
- N. Shpigel, M. D. Levi, S. Sigalov, L. Daikhin and D. Aurbach, *Acc. Chem. Res.*, 2018, 51, 69–79.
- 12 M. D. Levi, S. Sigalov, G. Salitra, P. Nayak, D. Aurbach, L. Daikhin, E. Perre and V. Presser, J. Phys. Chem. C, 2013, 117, 15505–15514.
- 13 M. Rodahl, F. Hook, A. Krozer, P. Brzezinski and B. Kasemoa, *Rev. Sci. Instrum.*, 1995, **66**, 3924–3930.
- 14 N. Shpigel, M. R. Lukatskaya, S. Sigalov, C. E. Ren, P. Nayak, M. D. Levi, L. Daikhin, D. Aurbach and Y. Gogotsi, ACS Energy Lett., 2017, 2, 1407–1415.
- 15 X. Qiao, X. Zhang, Y. Tian and Y. Meng, *Appl. Phys. Rev.*, 2016, 3, 031106.
- 16 L. Seidl, N. Bucher, E. Chu, S. Hartung, S. Martens, O. Schneider and U. Stimming, *Energy Environ. Sci.*, 2017, 10, 1631–1642.
- 17 K. Tomita, H. Noguchi and K. Uosaki, *ACS Appl. Energy Mater.*, 2018, **1**, 3434–3442.
- 18 D. Aurbach, M. Moshkovich, Y. Cohen and A. Schechter, *Langmuir*, 1999, **15**, 2947–2960.
- 19 Z.-W. Yin, X.-X. Peng, J.-T. Li, C.-H. Shen, Y.-P. Deng, Z.-G. Wu, T. Zhang, Q.-B. Zhang, Y.-X. Mo, K. Wang, L. Huang, H. Zheng and S.-G. Sun, ACS Appl. Mater. Interfaces, 2019, 11, 16214–16222.
- 20 K. Yang, Y. Li, L. Jia, Y. Wang, Z. Wang, Y. Ji, S. Yang, M. Titirici, X. Liu, L. Yang and F. Pan, *J. Energy Chem.*, 2021, 56, 438-443.
- 21 M. Nishizawa, T. Uchiyama, T. Itoh, T. Abe and I. Uchida, *Langmuir*, 1999, **15**, 4949–4951.
- 22 N. Serizawa, K. Shono, Y. Kobayashi, H. Miyashiro, Y. Katayama and T. Miura, *J. Power Sources*, 2015, **295**, 162–166.
- 23 S. Yagi, M. Fukuda, R. Makiura, T. Ichitsubo and E. Matsubara, *J. Mater. Chem. A*, 2014, 2, 8041.

Chem Soc Rev **Tutorial Review**

- 24 P. Jiménez, E. Levillain, O. Alévêque, D. Guyomard, B. Lestriez and J. Gaubicher, Angew. Chem., Int. Ed., 2017, 56, 1553-1556.
- 25 J. T. Li, S. R. Chen, X. Y. Fan, L. Huang and S. G. Sun, Langmuir, 2007, 23, 13174-13180.
- 26 H. Su, C. Fu, Y. Zhao, D. Long, L. Ling, B. M. Wong, J. Lu and J. Guo, ACS Energy Lett., 2017, 2, 2591-2597.
- 27 V. Singh, A. K. Padhan, S. D. Adhikary, A. Tiwari, D. Mandal and T. C. Nagaiah, J. Mater. Chem. A, 2019, 7, 3018-3023.
- 28 Y. G. Ryu, S. Lee, S. Mah, D. J. Lee, K. Kwon, S. Hwang and S. Doo, J. Electrochem. Soc., 2008, 155, A583-A589.
- 29 N. Nitta, F. Wu, J. T. Lee and G. Yushin, Mater. Today, 2015, 18, 252-264.
- 30 S. Sevinc, B. Tekin, A. Ata, M. Morcrette, H. Perrot, O. Sel and R. Demir-Cakan, I. Power Sources, 2019, 412, 55-62.
- 31 D. Aurbach and M. Moshkovich, J. Electrochem. Soc., 1998, 145, 2629-2639.
- 32 K. S. Smaran, S. Shibata, A. Omachi, A. Ohama, E. Tomizawa and T. Kondo, J. Phys. Chem. Lett., 2017, 8, 5203-5208.
- 33 F. Ding, W. Xu, X. Chen, J. Zhang, Y. Shao, M. H. Engelhard, Y. Zhang, T. A. Blake, G. L. Graff, X. Liu and J.-G. Zhang, J. Phys. Chem. C, 2014, 118, 4043-4049.
- 34 L. Johnson, C. Li, Z. Liu, Y. Chen, S. A. Freunberger, P. C. Ashok, B. B. Praveen, K. Dholakia, J. M. Tarascon and P. G. Bruce, Nat. Chem., 2014, 6, 1091-1099.
- 35 D. G. Kwabi, M. Tulodziecki, N. Pour, D. M. Itkis, C. V. Thompson and Y. Shao-Horn, J. Phys. Chem. Lett., 2016, 7, 1204-1212.
- 36 D. Sharon, D. Hirsberg, M. Afri, F. Chesneau, R. Lavi, A. A. Frimer, Y. K. Sun and D. Aurbach, ACS Appl. Mater. Interfaces, 2015, 7, 16590-16600.
- 37 D. Sharon, V. Etacheri, A. Garsuch, M. Afri, A. A. Frimer and D. Aurbach, J. Phys. Chem. Lett., 2013, 4, 127-131.
- 38 W. R. Torres, L. Cantoni, A. Y. Tesio, M. del Pozo and E. J. Calvo, J. Electroanal. Chem., 2016, 765, 45-51.
- 39 N. A. Galiote, D. C. de Azevedo, O. N. Oliveira and F. Huguenin, J. Phys. Chem. C, 2014, 118, 21995-22002.
- 40 W. R. Torres, F. Davia, M. del Pozo, A. Y. Tesio and E. J. Calvo, J. Electrochem. Soc., 2017, 164, A3785-A3792.
- 41 K. Xu, Chem. Rev., 2014, 114, 11503-11618.

- 42 D. Aurbach and A. Zaban, J. Electroanal. Chem., 1995, 393, 43-53.
- 43 H. Sonoki, M. Matsui and N. Imanishi, J. Electrochem. Soc., 2019, 166, A3593-A3598.
- 44 V. Dargel, N. Shpigel, S. Sigalov, P. Nayak, M. D. Levi, L. Daikhin and D. Aurbach, Nat. Commun., 2017, 8, 1389.
- 45 A. A. Hubaud, Z. Yang, D. J. Schroeder, F. Dogan, L. Trahey and J. T. Vaughey, J. Power Sources, 2015, 282, 639-644.
- 46 Z. Z. Yang, B. J. Ingram and L. Trahey, J. Electrochem. Soc., 2014, **161**, A1127-A1131.
- 47 Z. Yang, M. C. Dixon, R. A. Erck and L. Trahey, ACS Appl. Mater. Interfaces, 2015, 7, 26585-26594.
- 48 Z. Yang, A. A. Gewirth and L. Trahey, ACS Appl. Mater. Interfaces, 2015, 7, 6557-6566.
- 49 J. Zheng, Y. Hou, Y. Duan, X. Song, Y. Wei, T. Liu, J. Hu, H. Guo, Z. Zhuo, L. Liu, Z. Chang, X. Wang, D. Zherebetskyy, Y. Fang, Y. Lin, K. Xu, L. W. Wang, Y. Wu and F. Pan, Nano Lett., 2015, 15, 6102-6109.
- 50 P. Lemaire, T. Dargon, D. Alves Dalla Corte, O. Sel, H. Perrot and J. M. Tarascon, Anal. Chem., 2020, 92, 13803-13812.
- 51 D. Aurbach, A. Zaban, Y. Ein-Eli, I. Weissman, O. Chusid, B. Markovsky, M. Levi, E. Levi, A. Schechter and E. Granot, J. Power Sources, 1997, 68, 91-98.
- 52 Y. Choi, S. Pyun and H.-C. Shin, Met. Mater., 1998, 4, 193-201.
- 53 D. Shu, Y. Yang, X. Xia and Z. G. Lin, Chem. J. Chin. Univ., 1998, 19, 805-807.
- 54 H.-L. Wu, L. A. Huff, J. L. Esbenshade and A. A. Gewirth, ACS Appl. Mater. Interfaces, 2015, 7, 20820-20828.
- 55 S. Yagi, M. Fukuda, T. Ichitsubo, K. Nitta, M. Mizumaki and E. Matsubara, J. Electrochem. Soc., 2015, 162, A2356.
- 56 Y. Zhang, Y. Liang, H. Dong, X. Wang and Y. Yao, J. Electrochem. Soc., 2020, 167, 070558.
- 57 S. Yamagata, I. Takahara, M. Wang, T. Mizoguchi and S. Yagi, J. Alloys Compd., 2020, 846, 156469.
- 58 H. Jiang, W. Shin, L. Ma, J. J. Hong, Z. Wei, Y. Liu, S. Zhang, X. Wu, Y. Xu, Q. Guo, M. A. Subramanian, W. F. Stickle, T. Wu, J. Lu and X. Ji, Adv. Energy Mater., 2020, 10, 2000968.
- 59 S. Wang, F. Li, A. D. Easley and J. L. Lutkenhaus, Nat. Mater., 2019, 18, 69-75.